
Universiteit
Leiden
The Netherlands

The ESO Nearby Abell Cluster Survey. II. The distribution of velocity dispersions of rich galaxy clusters.

Mazure, A.; Katgert, P.; den Hartog, R.; Biviano, A.; Dubath, P.; Escalera, E.; ... ; Rhee, G.F.R.N.

Citation
Mazure, A., Katgert, P., Den Hartog, R., Biviano, A., Dubath, P., Escalera, E., ... Rhee, G. F. R. N. (1996). The ESO Nearby Abell Cluster Survey. II. The distribution of velocity dispersions of rich galaxy clusters. *Astronomy And Astrophysics*, *310*, 31-48. Retrieved from https://hdl.handle.net/1887/8478

Version: Not Applicable (or Unknown)
License:
Downloaded from: https://hdl.handle.net/1887/8478

Note: To cite this publication please use the final published version (if applicable).

1996A&A...310...31M

Astron. Astrophys. 310, 31–48 (1996)

ASTRONOMY AND ASTROPHYSICS

The ESO Nearby Abell Cluster Survey

II. The distribution of velocity dispersions of rich galaxy clusters*,**

A. Mazure[1], P. Katgert[2], R. den Hartog[2], A. Biviano[2,3], P. Dubath[4], E. Escalera[5,6], P. Focardi[7], D. Gerbal[3,8], G. Giuricin[5,9], B. Jones[10], O. Le Fèvre[8], M. Moles[11], J. Perea[11], and G. Rhee[12]

[1] Laboratoire d'Astronomie Spatiale, Marseille, France
[2] Sterrewacht Leiden, The Netherlands
[3] Institut d'Astrophysique de Paris, France
[4] Observatoire de Genève, Switzerland & Lick Observatory, Univ. of California, Santa Cruz, USA
[5] Dipartimento di Astronomia, Università di Trieste, Italy
[6] Royal Observatory, Edinburgh, UK
[7] Dipartimento di Astronomia, Università di Bologna, Italy
[8] DAEC, Observatoire de Paris, Université Paris 7, CNRS (UA 173), France
[9] SISSA, Trieste, Italy
[10] Nordita, Copenhagen, Denmark
[11] Instituto de Astrofísica de Andalucía, CSIC, Granada, Spain
[12] Department of Physics, University of Nevada, Las Vegas, USA

Received 22 January 1995 / Accepted 2 October 1995

Abstract. The ESO Nearby Abell Cluster Survey (the ENACS) has yielded 5634 redshifts for galaxies in the directions of 107 rich, Southern clusters selected from the ACO catalogue (Abell et al. 1989). By combining these data with another 1000 redshifts from the literature, of galaxies in 37 clusters, we construct a volume-limited sample of 128 $R_{\rm ACO} \geq 1$ clusters in a solid angle of 2.55 sr centered on the South Galactic Pole, out to a redshift $z = 0.1$. For a subset of 80 of these clusters we can calculate a reliable velocity dispersion, based on at least 10 (but very often between 30 and 150) redshifts.

We deal with the main observational problem that hampers an unambiguous interpretation of the distribution of cluster velocity dispersions, namely the contamination by fore- and background galaxies. We also discuss in detail the completeness of the cluster samples for which we derive the distribution of cluster velocity dispersions. We find that a cluster sample which is complete in terms of the field-corrected richness count given in the ACO catalogue gives a result that is essentially identical to that based on a smaller and more conservative sample which is complete in terms of an intrinsic richness count that has been corrected for superposition effects.

We find that the large apparent spread in the relation between velocity dispersion and richness count (based either on visual inspection or on machine counts) must be largely intrinsic; i.e. this spread is not primarily due to measurement uncertainties. One of the consequences of the (very) broad relation between cluster richness and velocity dispersion is that all samples of clusters that are defined complete with respect to richness count are unavoidably biased against low-σ_V clusters. For the richness limit of our sample this bias operates only for velocity dispersions less than ≈800 km/sec.

We obtain a statistically reliable distribution of global velocity dispersions which, for velocity dispersions $\sigma_V \gtrsim 800$ km/s, is free from systematic errors and biases. Above this value of σ_V our distribution agrees very well with the most recent determination of the distribution of cluster X-ray temperatures, from which we conclude that $\beta = \sigma_V^2 \mu m_H / kT_X \approx 1$.

The observed distribution $n(> \sigma_V)$, and especially its high-σ_V tail above ≈800 km/s, provides a reliable and discriminative constraint on cosmological scenarios for the formation of structure. We stress the need for model predictions that produce exactly the same information as do the observations, namely dispersions of line-of-sight velocity of galaxies within the turnaround radius and inside a cylinder rather than a sphere, for a sample of model clusters with a richness limit that mimics that of the sample of observed clusters.

Key words: galaxies: clusters of – galaxies: redshifts – cosmology: observations – dark matter

Send offprint requests to: A. Mazure

* Based on observations collected at the European Southern Observatory (La Silla, Chile)

** Tables 1a and 1b are also available in electronic form at the CDS via anonymous ftp 130.79.128.5

© European Southern Observatory • Provided by the NASA Astrophysics Data System

1996A&A...310...31M

1. Introduction

The present-day distribution of cluster masses contains information about important details of the formation of large-scale structure in the Universe. In principle, the distribution of present cluster masses constrains the form and amplitude of the spectrum of initial fluctuations, via the tail of high-amplitude fluctuations from which the clusters have formed, as well as the cosmological parameters that influence the formation process. Recently, several authors have attempted to use either the distribution of cluster mass estimates, or of gauges of the mass (such as the global velocity dispersion, or the temperature of the X-ray gas) to constrain parameters in cosmological scenarios. For example, Frenk et al. (1990, FWED hereafter) have attempted to constrain the bias parameter required by the CDM scenario through a comparison of their predictions from N-body simulations with the observed distribution of cluster velocity dispersions and X-ray temperatures. Subsequently, Henry & Arnaud (1991) have used the distribution of cluster X-ray temperatures to constrain the slope and the amplitude of the spectrum of fluctuations. More recently, Bahcall & Cen (1992), Biviano et al. (1993), and White et al. (1993) have used the distribution of estimated masses to constrain the cosmological density parameter, the power-spectrum index, as well as the bias parameter.

For constraining the *slope* of the spectrum of initial fluctuations through the slope of the mass distribution, unbiased estimates of the mass (or of a relevant mass gauge) are required. The latter always require assumptions about either the shape of the galaxy orbits, the shape of the mass distribution, or about the distribution of the gas temperature. Therefore gauges of the total mass that are based on directly observable parameters, such as global velocity dispersions or central X-ray temperatures, are sometimes preferable. However, the use of such mass gauges also requires a lot of care. Global velocity dispersions, although fairly easily obtained, can be affected by projection effects and contamination by field galaxies, as discussed by e.g. FWED. In addition, velocity dispersions may depend on the size of the aperture within which they are determined, because the dispersion of the line-of-sight velocities often varies with distance from the cluster centre (e.g. den Hartog & Katgert 1995).

More fundamentally, the velocity dispersion of the galaxies may be a biased estimator of the cluster potential (or mass) as a result of dynamical friction and other relaxation processes. In principle, the determination of the X-ray temperatures is more straightforward. However, temperature estimates may be affected by cooling flows, small-scale inhomogeneities (Walsh & Miralda-Escudé 1995), bulk motions or galactic winds (Metzler & Evrard 1994). Also, temperature estimates of high accuracy require high spectral resolution and are therefore less easy to obtain.

To obtain useful constraints on the *amplitude* of the fluctuation spectrum, it is essential that the completeness of the cluster sample in the chosen volume is accurately known. The completeness of cluster samples constructed from galaxy catalogues obtained with automatic scanning machines, such as the COSMOS and APM machines (see e.g. Lumsden et al. 1992, LNCG hereafter, and Dalton et al. 1992) is, in principle, easier to discuss than that of the ACO catalogue, which until recently was the only source of cluster samples. In theory, one is primarily interested in the completeness with respect to a well-defined limit in mass. In practice, cluster samples based on optical catalogues can be defined only with respect to richness, and the relation between richness and mass seems to be very broad. A further complication is that all optical cluster catalogues suffer from superposition effects, which can only be resolved through extensive spectroscopy. Cluster samples based on X-ray surveys do not suffer from superposition effects, but they are (of necessity) flux-limited, and the extraction of volume-limited samples with well-defined luminosity limits requires follow-up spectroscopy (e.g. Pierre et al. 1994). The large spread in the relation between X-ray luminosity and X-ray temperature (e.g. Edge & Stewart 1991) implies that, as with the optical samples, the construction of cluster samples with a well-defined mass limit from X-ray surveys is not at all trivial.

In this paper we discuss the distribution of velocity dispersions, for a volume-limited sample of rich ACO clusters with known completeness. The discussion is based on the results of our ESO Nearby Abell Cluster Survey (ENACS, Katgert et al. 1995, hereafter Paper I), which has yielded 5634 reliable galaxy redshifts in the direction of 107 rich, nearby ACO clusters with redshifts out to about 0.1. We have supplemented our data with about 1000 redshifts from the literature for galaxies in 37 clusters.

In Sect. 2 we describe the construction of a volume-limited sample of rich clusters. In Sect. 3 we discuss superposition effects, and introduce a *3-dimensional* richness (derived from Abell's projected, 2-dimensional richness). In Sect. 4 we discuss the completeness of the cluster sample, and we estimate the spatial density of rich clusters. In Sect. 5 we summarize the procedure that we used for eliminating interlopers, which is essential for obtaining unbiased estimates of velocity dispersion. In Sect. 6 we derive the properly normalized distribution of velocity dispersions. In Sect. 7 we compare our distribution with earlier results from the literature, which include both distributions of velocity dispersions and of X-ray temperatures. Finally, we also compare our result with some published predictions from N-body simulations.

2. The cluster sample

2.1. Requirements

The observational determination of the distribution of cluster velocity dispersions, $n(\sigma_V)$, requires a cluster sample that is either not biased with respect to σ_V, or that has a bias which is sufficiently well-known that it can be corrected for in the observations or be accounted for in the predictions. If this condition is fulfilled for a certain range of velocity dispersions, the *shape* of the distribution can be determined over that range. A determination of the *amplitude* of the distribution requires that the spatial completeness of the cluster sample is also known.

© European Southern Observatory • Provided by the NASA Astrophysics Data System

1996A&A...310...31M

Until complete galaxy redshift surveys over large solid angles and out to sufficiently high redshifts become available, it will not be possible to construct cluster samples that are complete to a well-defined limit in velocity dispersion. The only possible manner in which this ideal can at present be approached is by selecting cluster samples from catalogues that are based on overdensities in projected distributions of galaxies (or in X-ray surface brightness). By selecting only the clusters with an apparent richness (i.e. surface density in a well-defined range of absolute magnitudes) above a certain lower limit, one may hope to obtain an approximate lower limit in intrinsic richness (i.e. with fore- and background-galaxies removed).

By virtue of the general (but very broad) correlation between richness and velocity dispersion one can then expect to achieve completeness with respect to velocity dispersion above a lower limit in σ_V. Below that limit the cluster sample will be inevitably incomplete with respect to velocity dispersion, in a manner that is specific for the adopted richness limit. In other words: observed and predicted velocity dispersion distributions can be compared directly above the limiting σ_V set by the richness limit. For smaller values of the velocity dispersion the prediction should take into account the bias introduced by the particular richness limit.

2.2. *The southern ACO $R \geq 1$ cluster sample*

The ENACS was designed to establish, in combination with data already available in the literature, a database for a complete sample of $R \geq 1$ ACO clusters, out to a redshift of $z = 0.1$, in a solid angle of 2.55 sr around the SGP, defined by $b \leq -30°$ and $-70° \leq \delta \leq 0°$ (a volume we will refer to as the 'cone'). For our sample we selected clusters which at the time either had a known spectroscopic redshift $z \leq 0.1$, or which had $m_{10} \leq 16.9$. Judging from the $m_{10} - z$ relation the clusters with $m_{10} \leq 16.9$ should include most of the $z \leq 0.1$ clusters. With this selection, the contamination from $z > 0.1$ clusters would clearly be non-negligible due to the spread in the $m_{10} - z$ relation.

At present, after completion of our project and with other new data in the literature, the region defined above contains 128 $R \geq 1$ ACO clusters with a measured or estimated redshift $z \leq 0.1$. A spectroscopically confirmed redshift $z \leq 0.1$ is available for 122 clusters, while for the remaining 6 a redshift ≤ 0.1 has been estimated on the basis of photometry. The redshift values (or estimates), if not from the ENACS, were taken from Abell et al. (1989), Struble & Rood (1991), Peacock and West (1992, and private communication), Postman et al. (1992), Dalton et al. (1994) and Quintana & Ramírez (1995).

We will show below that the 128 clusters form a sample that can be used for statistical analysis. Of the 122 redshift surveys of clusters with $z \leq 0.1$ in the specified region, 78 were contributed to by the ENACS, either exclusively or in large measure. In 80 of the 122 redshift surveys we find at least one system with 10 or more member galaxies. Of the latter 80 surveys, 68 were contributed to by our survey.

In Table 1a we list several properties of the main systems in the direction of the 128 clusters (in the 'cone' and with $z < 0.1$)

Table 1a. The statistical sample of 128 ACO clusters that are in the 'cone' and have a main system with $z < 0.1$, and 14 relevant secondary systems with $z < 0.1$.

ACO	$N_{\rm mem}$	z	σ_V^c	$C_{\rm ACO}$	$C_{\rm bck}$	$C_{\rm 3D}$
A0013	37	0.0943	886	96	20.7	98.2
A0074‡	5	0.0654	-	50	15.0	-
A0085‡	116	0.0556	853	59	15.9	55.9
	17	0.0779	462	59	15.9	7.7
A0087	27	0.0550	859	50	24.3	47.8
A0119†	125	0.0442	740	69	17.5	76.1
A0126‡	1	0.0850	-	51	24.3	-
A0133‡	9	0.0566	-	60	15.8	-
A0151†	63	0.0533	669	72	17.5	39.1
	40	0.0997	857	72	17.5	25.2
	29	0.0410	395	72	17.5	18.3
A0168	76	0.0450	517	89	16.5	80.2
A0261‡	1	0.0467	-	63	30.5	-
A0277‡	2	0.0927	-	50	16.1	-
A0295	30	0.0426	297	51	24.3	52.6
A0303	4	0.0595	-	50	24.3	18.6
A0367	27	0.0907	963	101	19.5	108.4
A0415‡	1	0.0788	-	67	20.8	-
A0420	19	0.0858	514	55	26.3	46.8
A0423‡	2	0.0795	-	89	24.3	-
A0484‡	4	0.0386	-	50	27.3	-
A0496‡	134	0.0328	682	50	16.8	57.0
A0500‡	1	0.0666	-	58	17.2	-
A0514	82	0.0713	874	78	14.5	68.4
A0524	26	0.0779	822	74	34.4	65.6
	10	0.0561	211	74	34.4	25.3
A2361	24	0.0608	329	69	27.3	70.0
A2362	17	0.0608	340	50	25.3	47.4
A2377‡	1	0.0808	-	94	27.3	-
A2382‡	1	0.0648	-	50	17.7	-
A2384‡	1	0.0943	-	72	24.8	-
A2399‡	1	0.0587	-	52	16.1	-
A2400‡	1	0.0881	-	56	23.1	-
A2401	23	0.0571	472	66	18.6	64.9
A2410‡	1	0.0806	-	54	17.7	-
A2420‡	1	0.0838	-	88	26.3	-
A2426	15	0.0978	846	114	26.3	58.5
	11	0.0879	313	114	26.3	42.9
A2436	14	0.0914	530	56	27.3	61.4
A2480	11	0.0719	862	108	23.0	80.0
A2492‡	2	0.0711	-	62	18.6	-
A2500	13	0.0895	477	71	82.2	55.3
	12	0.0783	283	71	82.2	51.0
A2502‡	0	0.0972	-	58	24.3	-
A2528‡	1	0.0955	-	73	22.0	-
A2538‡	42	0.0832	861	83	19.1	95.3
A2556‡	2	0.0865	-	67	21.2	-
A2559‡	1	0.0796	-	73	28.3	-
A2566‡	1	0.0821	-	67	28.4	-
A2569	36	0.0809	481	56	24.3	70.5
A2599‡	1	0.0880	-	84	16.2	-
A2638‡	1	0.0825	-	123	30.5	-
A2644	12	0.0688	259	59	24.3	28.6

© European Southern Observatory • Provided by the NASA Astrophysics Data System

1996A&A...310...31M

Table 1a. (continued)

ACO	N_{mem}	z	σ_V^c	C_{ACO}	C_{bck}	C_{3D}
A2670‡	219	0.0762	908	142	15.9	114.1
A2717†	56	0.0490	512	52	10.8	43.4
A2734	77	0.0617	581	58	12.3	45.9
A2755	22	0.0949	789	120	28.2	90.6
A2764	19	0.0711	788	55	19.6	59.1
A2765	16	0.0801	905	55	47.7	58.7
A2799	36	0.0633	424	63	20.2	71.3
A2800	34	0.0636	430	59	18.6	57.4
A2819	50	0.0747	406	90	23.8	45.2
	44	0.0867	359	90	23.8	39.7
A2854	22	0.0613	369	64	28.1	58.0
A2889‡	1	0.0667	-	65	22.0	-
A2911	31	0.0808	576	72	21.3	65.7
A2915	4	0.0864	-	55	25.0	-
A2923	16	0.0715	339	50	42.3	44.8
A2933	9	0.0925	-	77	28.2	86.1
A2954	6	0.0566	-	121	32.2	38.3
A2955‡	0	0.0989	-	56	34.4	-
A3009	12	0.0653	514	54	21.3	56.5
A3040‡	1	0.0923	-	69	17.2	-
A3093	22	0.0830	435	93	22.5	63.5
A3094	66	0.0672	653	80	18.6	65.8
A3107‡	0	0.0875	-	61	20.4	-
A3108	7	0.0625	-	73	30.5	51.7
	5	0.0819	-	73	30.5	36.9
A3111	35	0.0775	770	54	18.6	52.9
A3112	67	0.0750	950	116	25.2	92.8
A3122	87	0.0643	755	100	21.4	88.7
A3126‡	38	0.0856	1041	75	29.3	88.1
A3128†	180	0.0599	802	140	19.4	129.3
	12	0.0395	386	140	19.4	8.6
	12	0.0771	103	140	19.4	8.6
A3135‡	1	0.0633	-	111	28.6	-
A3144	1	0.0423	-	54	16.3	-
A3151	34	0.0676	747	52	23.8	60.0
A3152‡	0	0.0891	-	51	26.0	-
A3153‡	0	0.0958	-	64	26.0	-
A3158	105	0.0591	1005	85	10.8	82.5
A3194	32	0.0974	790	83	13.3	93.5
A3202	27	0.0693	433	65	28.1	61.3
A3223	68	0.0601	636	100	14.2	69.6
A3264	5	0.0978	-	53	37.6	41.2
A3266‡	158	0.0589	1105	91	19.0	97.1
A3301	5	0.0536	-	172	7.3	-
A3330‡	1	0.0910	-	52	18.0	-
A3334‡	32	0.0965	671	82	29.3	86.9
A3341	63	0.0378	566	87	23.9	59.2
	15	0.0776	751	87	23.9	14.1
A3351‡	0	0.0819	-	114	35.0	-
A3360‡	36	0.0848	801	85	34.6	107.7
A3651	78	0.0599	661	75	33.2	91.8
A3667†	162	0.0556	1059	85	33.2	85.1
A3677	8	0.0912	-	60	25.0	37.7
A3682	10	0.0921	863	66	41.1	97.3
A3691	33	0.0873	792	115	40.9	142.9

Table 1a. (continued)

ACO	N_{mem}	z	σ_V^c	C_{ACO}	C_{bck}	C_{3D}
A3693	16	0.0910	585	77	25.0	49.5
A3695	81	0.0893	845	123	39.5	137.2
A3696	12	0.0882	428	58	30.6	88.6
A3698‡	1	0.0198	-	71	7.7	-
A3703	18	0.0735	455	52	27.3	44.6
	13	0.0914	697	52	27.3	32.2
A3705	29	0.0898	1057	100	32.0	93.3
A3716‡	65	0.0448	781	66	11.6	61.6
A3733	41	0.0389	696	59	4.7	59.4
A3744	66	0.0381	559	70	10.5	62.8
A3764	38	0.0757	671	53	24.0	68.1
A3781	4	0.0571	-	79	16.2	25.4
	4	0.0729	-	79	16.2	25.4
A3795	13	0.0890	336	51	31.9	77.0
A3799	10	0.0453	428	50	24.9	50.0
A3806	84	0.0765	813	115	11.7	89.4
A3809	89	0.0620	499	73	20.8	55.5
A3822	84	0.0759	969	113	22.5	112.8
A3825	59	0.0751	698	77	12.0	58.4
A3826‡	1	0.0754	-	62	13.2	-
A3827	20	0.0984	1114	100	28.4	116.7
A3844‡	1	0.0730	-	52	23.0	-
A3879	46	0.0669	516	114	39.5	85.0
A3897	10	0.0733	548	63	21.3	64.8
A3911‡	1	0.0960	-	58	30.5	-
A3921	32	0.0936	585	93	25.0	99.3
A3969‡	1	0.0699	-	55	40.5	-
A4008	27	0.0549	424	66	36.0	64.1
A4010	30	0.0957	615	67	28.2	79.3
A4038‡	51	0.0292	839	117	17.1	110.4
A4053	17	0.0720	731	64	16.2	43.9
	9	0.0501	-	64	16.2	23.2
A4059‡	10	0.0488	526	66	11.0	69.9
A4067‡	30	0.0989	719	72	30.5	75.0

Notes: col.(1): A dagger indicates a combination of data from the ENACS and from the literature, a double dagger indicates that only data from the literature were used; col.(2): secondary systems are listed if they contain either $\geq$10 redshifts or $\geq$50% of the number of redshifts of the main system; col.(3): redshift values (or photometric estimates, indicated by N_z=0) of clusters for which no ENACS data exist, were taken from Abell et al. (1989), Struble & Rood (1991), Dalton et al. (1994), Postman et al. (1992), West (private communication) and Quintana & Ramírez (1995)

that constitute the sample on which we will base our discussion of the distribution of cluster velocity dispersions, as well as the properties of 14 subsystems with $z < 0.1$ that either have 10 redshifts or at least half the number of redshifts in the main system. In Table 1b we list the same type of data for the other systems described in Paper I, with at least 10 members so that a velocity dispersion could be determined. As the latter are outside the 'cone' defined above (or have $z > 0.1$), they have not been used in the present discussion but could be useful for other

© European Southern Observatory • Provided by the NASA Astrophysics Data System

1996A&A...310...31M

Table 1b. Main systems in the 'cone' with $z > 0.1$ and $N \geq 10$ (with relevant secondary systems), and systems outside the 'cone' with $N \geq 10$.

ACO	N_{mem}	z	σ_V^c	C_{ACO}	C_{bck}	C_{3D}
A0118	30	0.1148	649	77	35.8	89.1
A0229	32	0.1139	856	77	24.3	83.1
A0380	25	0.1337	703	82	35.8	71.8
A0543	10	0.0850	413	90	244.2	139.3
A0548†	323	0.0416	842	92	12.2	88.4
	21	0.1009	406			5.4
	15	0.0868	1060			3.9
A0754†	90	0.0543	749	92	17.0	101.6
A0957	34	0.0447	741	55	16.8	67.8
A0978	56	0.0544	498	55	16.1	61.4
A1069	35	0.0650	1120	45	17.2	54.5
A1809†	58	0.0791	702	78	16.0	81.7
A2040	37	0.0461	673	52	15.9	58.4
A2048	25	0.0972	668	75	17.7	59.4
A2052†	62	0.0350	655	41	17.5	52.5
A2353	24	0.1210	599	51	26.3	59.8
A2715*	14	0.1139	556	112	30.5	58.7
A2778	17	0.1018	947	51	11.9	26.7
	10	0.1182	557			15.7
A2871	18	0.1219	930	92	48.0	63.0
	14	0.1132	319			49.0
A3141	15	0.1058	646	55	16.2	48.5
A3142*	21	0.1030	814	78	13.0	50.3
	12	0.0658	785			28.7
A3354	57	0.0584	383	54	9.8	33.6
A3365	32	0.0926	1153	68	32.0	91.5
A3528	28	0.0526	969	70	6.2	54.7
A3558†	328	0.0479	939	226	8.7	127.0
A3559	39	0.0461	443	141	9.3	85.0
	11	0.1119	537			24.0
A3562	114	0.0490	1048	129	12.6	140.4
A3864	32	0.1033	940	60	29.5	69.8

Notes: col.(1): an asterisk indicates that the system is in the 'cone', a dagger indicates a combination of data from the ENACS and from the literature; col.(2): secondary systems are listed if they contain either $\geq$10 redshifts or $\geq$50% of the number of redshifts of the main system

A description of the ways in which the data in Tables 1a and 1b have been obtained will be given in the next sections.

3. Superposition effects in the ACO cluster catalogue

It is clear from the redshift distributions towards our target clusters in the ENACS (see Fig. 7 in Paper I) that for most clusters in the $R_{ACO} \geq 1$ sample the fraction of fore- and background galaxies is non-negligible.

In Paper I we have discussed how one can identify the fore- and background galaxies, namely as the 'complement' of the galaxies in the physically relevant systems. In order to identify the latter, we used a fixed velocity gap to decide whether two galaxies in the survey that are adjacent in redshift, are part of the same system or of two separate systems. The minimum velocity difference that defines galaxies to be in separate systems was determined for the ENACS from the sum of the 107 distributions of the velocity gap between galaxies that are adjacent in velocity. We found that a gap-width of 1000 km/s is sufficient to identify systems, that it does not break up systems inadvertently, and is conservative in the sense that it does not eliminate outlying galaxies of a system. Note that the gap-size of 1000 km/s is geared to the sampling in our survey and to the average properties of the redshift systems; for other datasets the required gap-size may be different. The systems that result from applying this procedure to the ENACS data are given in Table 6 of Paper I.

Having identified the systems in the redshift surveys of our clusters we can quantify the effect of the superposition of fore- and background galaxies on the ACO richness estimates. Our observing strategy has been to obtain, for the target clusters, redshifts for the N brightest galaxies in a field consisting of 1 to 3 circular apertures with a diameter of $\approx 0.5°$. For most clusters in our programme this corresponds roughly to the size of the field in which the richness count was determined. We can therefore estimate an intrinsic '3-D' richness of a cluster as the product of the fraction f_{main} of galaxies that reside in the main system (i.e. in the system with the largest number of members) with the *total* galaxy count obtained by Abell et al. (1989).

The total count is not available in the ACO catalogue and must be recovered as the sum of the corrected count C_{ACO} published by Abell et al. (1989) and the correction for the contribution of the field, C_{bck}, that they subtracted from their measured total count. The intrinsic 3-D richness thus follows as $C_{3D} = f_{main} \times (C_{ACO} + C_{bck})$, in which we replace the statistical field corrections of Abell et al. (1989) (based on integrals of the galaxy luminosity function) by field corrections based on redshift surveys. The first ingredient in the calculation of the intrinsic 3 - D richness is f_{main}. In Fig. 1a we show the distribution of the fraction f_{main} for the 80 redshift surveys with $N \geq 10$ and $z \leq 0.1$ in our sample. We estimated f_{main} only for systems with at least 10 measured redshifts, because for $N < 10$ the definition of systems is not very stable, so that the determination of f_{main} is likewise not very reliable. According to Girardi et al. (1993), the minimum number of galaxies required to obtain a reliable estimate of σ_V also happens to be about 10. We find that, on average, $\approx 73\%$ of the galaxies in our redshift surveys towards $R_{ACO} \geq 1$ clusters with $z \lesssim 0.1$ belongs to the main system.

The correction C_{bck}, which accounts for the contribution of the field to the total count, was derived as follows. Abell et al. (1989) describe a parametrization of the background correction, which is the number of field galaxies down to a limiting magnitude of $m_3 + 2$ (the limit of the uncorrected richness count), in the same aperture in which the total count was made. The latter has a diameter that is based on the estimated distance through the $m_{10} - z$ relation. To calculate C_{bck} for a cluster, it is thus necessary to have its m_3 and m_{10}. These parameters are known for those 65 of the 80 clusters in our sample that are in the southern part of the ACO catalogue. The other 15 clusters were

© European Southern Observatory • Provided by the NASA Astrophysics Data System

1996A&A...310...31M

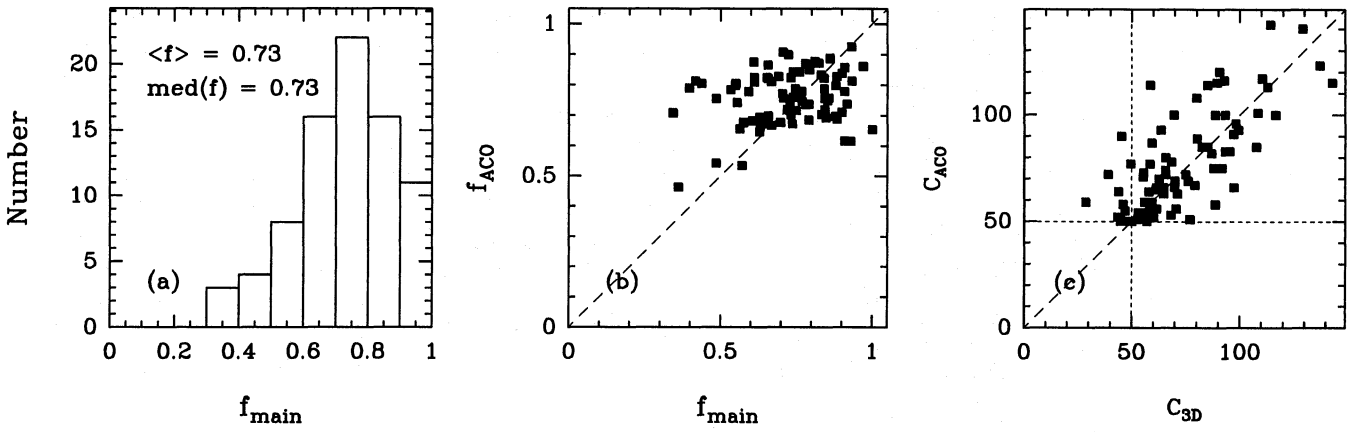

Fig. 1. a The distribution of f_{main}, the fraction of galaxies in the largest system (determined from redshift surveys), for the 80 systems with $N \geq 10$ and $z \leq 0.1$. **b** The relation between f_{ACO} (= $C_{ACO}/(C_{ACO} + C_{bck})$) and f_{main}. **c** The relation between C_{ACO} and C_{3D} = $f_{main} \times (C_{ACO} + C_{bck})$; the horizontal dashed line indicates C_{ACO} = 50, the vertical dashed line C_{3D} = 50.

described by Abell (1958), who did not use a parametrized estimate of the background, nor did he list m_3. Instead, he estimated C_{bck} by counting all galaxies down to $m_3 + 2$ in a field near each cluster that clearly did not contain another cluster. To recover an approximate value of C_{bck} for these 15 clusters we first estimated m_3 from m_{10}. Using 97 $R \geq 1$ clusters in our sample out to $z = 0.1$ we found $m_3 = 0.987\, m_{10} - 0.608$, with a spread of 0.30 mag. Finally, we used the parametrization of Abell et al. (1989) for these 15 clusters to calculate C_{bck} (which should be very close but need not identical to the value subtracted by Abell).

In Fig. 1b we show the relation between f_{main} and f_{ACO}(= $C_{ACO}/(C_{ACO} + C_{bck})$. The average and median values of f_{ACO} are both 0.76, i.e. practically identical to the corresponding values for f_{main}. So, *on average*, the field correction C_{bck} applied by Abell et al. (1989) was almost the same as the field correction we derive from our redshift surveys. However, f_{main} spans a much wider range than does f_{ACO}. It thus appears that the field correction of Abell et al. (1989) has probably introduced a considerable noise in the field-corrected richness estimates. The reason for this is that their correction was based on an 'average field', while for an individual cluster the actual field may differ greatly from the average.

This conclusion is supported by the data in Fig. 1c, where we show the relation between C_{ACO}, the count corrected for the model field contribution according to Abell et al. (1989), and C_{3D}, the intrinsic 3-D count calculated using f_{main}, which thus takes into account the actual field contamination for each cluster individually. Statistically, C_{ACO} and C_{3D} appear to measure the same quantity, i.e. the field correction of Abell et al. (1989) is, *on average*, in very good agreement with our estimates from the redshift surveys. However, the variations in the real field with respect to the average field must be mainly responsible for the very large spread in the values of C_{3D} for a fixed value of C_{ACO}. As the distribution of points in Fig.1 c seems to be very symmetric around the C_{ACO} = C_{3D} -line, we will later assume that the statistical properties of a complete cluster sample with $C_{ACO} \geq 50$ are not different from those of a sample with $C_{3D} \geq 50$.

For an individual cluster, C_{3D} is obviously a much more meaningful parameter than C_{ACO}. Yet, one has to be aware of possible systematic effects that may affect its use. First, as C_{3D} involves f_{main} any bias in the determination of f_{main} could also enter C_{3D}. The number of unrelated fore- and background galaxies is likely to depend on the redshift of a cluster, and therefore f_{main} might depend on redshift. However, as is evident from Fig. 2a, there is hardly any indication in our data that this is the case. At most, there may be a tendency for a slight bias against low values of f_{main} at the lowest redshifts. This is consistent with the fact that for the nearest clusters the field contribution is low and may not be very easy to determine properly. In principle, a slight bias against low values of f_{main} could result in a slight bias against low values of C_{3D} for nearby clusters. But, as can be seen from Fig. 2b, there is no indication that for nearby clusters the C_{3D} values are higher than average.

Secondly, there is a general tendency to select preferentially the richer clusters at higher redshifts, and a bias could therefore exist against the less rich systems at higher redshifts. Although the systems with the highest values of C_{3D} are indeed found near our redshift limit, there is no evidence in Fig. 2b that there is a strong bias against systems with $C_{3D} \approx 50$ near the redshift limit.

Thirdly, the full problem of the superposition of two rich systems along the line of sight is not appreciated in the simple definition of C_{3D}, and it is certainly possible that if two $R_{ACO} \geq 1$ systems are observed in superposition the most distant one may not be recognized as such. Fortunately, the probability of such a situation to occur is low. As is clear from Fig. 2c, there is no tendency for clusters with a high total count $C_{ACO} + C_{bck}$ to have a smaller value of f_{main}, as would be expected if superposition contributed significantly to the richness. As a matter of fact, given the density of $R \geq 1$ clusters (see next Sect.), we expect that for our sample of 128 clusters there is a probability of about 1% that a superposition of two $R \geq 1$ clusters occurs

© European Southern Observatory • Provided by the NASA Astrophysics Data System

1996A&A...310...31M

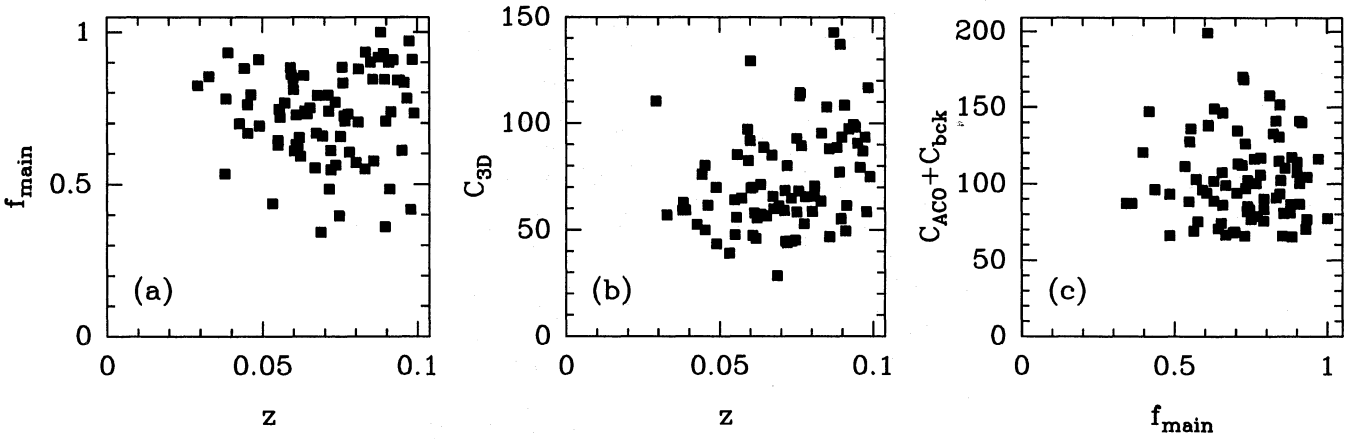

Fig. 2. a The dependence of $f_{\rm main}$ (the fraction of galaxies in the largest system) on the redshift of the main system. **b** The dependence of intrinsic richness count C_{3D} on the redshift of the system. **c** The dependence of $C_{ACO} + C_{bck}$ on $f_{\rm main}$.

in our data. This is consistent with the fact that in only one case, viz. that of A2500, we observe a secondary system with a value of $C_{3D} > 50$.

In principle, the sample of clusters with $C_{3D} \geq 50$ is to be preferred over the one with $C_{ACO} \geq 50$, as in the former the effects of superposition have been accounted for in a proper way. However, C_{3D} cannot be used as the main selection criterion for a cluster sample, because it requires $f_{\rm main}$ to be available for all clusters. From Fig. 1c it appears that, in a statistical sense, a cluster sample with $C_{ACO} \geq 50$ can be used as a substitute for a sample with $C_{3D} \gtrsim 50$ as, apart from the large scatter, the two richnesses are statistically equivalent. As a result of the large scatter in Fig. 1c, one can define a subsample of clusters from the $C_{ACO} \geq 50$ sample that is complete in terms of C_{3D} only if one limits the subsample to systems with $C_{3D} \geq 75$.

4. The completeness of the sample and the density of rich clusters

In the following discussion and in the remaining sections of this paper we will use the term "cluster" to refer to the main system in Table 1a, i.e. the system with the largest number of redshifts in each pencil beam, unless we explicitly state otherwise. Hence, the 14 secondary systems in Table 1a are not included, nor are the systems in Table1b, as the latter are not in the 'cone' defined in Sect. 2.2, or have $z > 0.1$.

We have estimated the completeness of our cluster sample with respect to redshift from the distribution of the number of clusters in 10 concentric shells, each with a volume equal to one-tenth of the total volume out to $z = 0.1$. The result is shown in Fig. 3. The dashed line shows the distribution for all 128 $C_{ACO} \geq 50$ clusters out to a redshift of 0.1. The solid line represents the subset of 80 clusters with at least 10 redshifts (for which a velocity dispersion is therefore available). Finally, the dotted line shows the distribution for the subset of 33 clusters with $N \geq 10$ *and* $C_{3D} \geq 75$. Note that in Table 1a there are 34 clusters with $C_{3D} \geq 75$ but one of these, A2933, has only 9 redshifts in the main system, whereas the total number of redshifts measured was sufficient to estimate $f_{\rm main}$ and, hence, C_{3D}.

From Fig. 3 it appears that the sample of 128 clusters with $C_{ACO} \geq 50$ has essentially uniform density, except for a possible ($\approx 2\sigma$) 'excess' near $z = 0.06$, and an apparent 'shortage' of clusters in the outermost bins. The 'excess' is at least partly due to the fact that several of the clusters in the Horologium-Reticulum and the Pisces-Cetus superclusters are in our cluster sample (see Paper I). As we will discuss in detail in the next Sect., the 'shortage' towards $z = 0.1$ is probably due to a combination of two effects. Firstly, some clusters that should have been found by Abell et al. to have $R_{ACO} \geq 1$ and $m_{10} \leq 16.9$ were not. Secondly, near the redshift limit of our sample Galactic obscuration may have caused some clusters to be excluded from the sample that they do belong to.

The subset of 80 clusters for which at least 10 redshifts are available appears to have essentially uniform density in the inner half of the volume, but a significantly lower density in the outer half. This apparent decrease is due to the fact that, for obvious reasons, the average number of *measured* redshifts decreases with increasing redshift; so much so that for $z \gtrsim 0.08$ the fraction of clusters with less than 10 redshifts is about 40%. Finally, the density of the subset of 33 clusters with $C_{3D} \geq 75$ appears constant out to a redshift of 0.1. This is consistent with the fact that none of the selection effects that operate for the two other samples are expected to affect the richest clusters.

4.1. The sample of 128 slusters with $R_{ACO} \geq 1$

In constructing our 'complete' sample, we have applied a limit $m_{10} \leq 16.9$ for the cluster candidates without a spectroscopic redshift. This limit was chosen so that we would include essentially all clusters with $z < 0.1$. It is possible that a few clusters have been missed, but it is very difficult to estimate from first principles how many clusters with $z \leq 0.1$ have been missed due to the m_{10} limit, and we will not try to make a separate estimate for this effect. However, it is important to realize that

© European Southern Observatory • Provided by the NASA Astrophysics Data System

1996A&A...310...31M

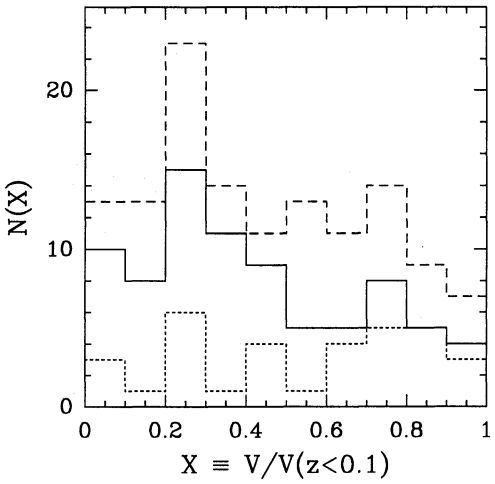

Fig. 3. The number of clusters in 10 concentric shells, each with a volume equal to one-tenth of the total volume out to $z = 0.1$. The ordinate is volume expressed as a fraction of the total volume out to $z = 0.1$. The dashed line represents all 128 clusters in the sample, the solid line the 80 clusters with $N \geq 10$, and the dotted line the 33 clusters with $C_{3D} \geq 75$.

the few clusters that we may have missed as a result of the m_{10} limit are unlikely to have $z < 0.08$.

It is possible that some clusters that should have been included were either not recognized by Abell (1958) or Abell et al. (1989), or have had their richness underestimated and have thus not made it into our sample. To a large extent, the magnitude of this effect can be estimated from a comparison with cluster catalogues based on machine scanning of plates. Below, we will describe such an estimate. As with the m_{10} limit, it is likely that clusters that have been missed for this reason are mostly in the further half of the volume.

Recently, two cluster catalogues that are based on galaxy catalogues obtained with machine scans of photographic plates have become available, namely the Edinburgh-Durham Cluster Catalogue (EDCC) by LNCG, and the APM cluster catalogue by Dalton et al. (1992). We now proceed to estimate, from a comparison with the EDCC, how many clusters with $R_{ACO} \geq 1$ (or $C_{ACO} \geq 50$) and $m_{10} \leq 16.9$ may have been missed by Abell et al. (1989).

In the following we will assume that the $C_{ACO} \geq 50$ criterion translates into a limit of $C_{EDCC} \geq 30$ in the EDCC richness count. This assumption is supported by several pieces of evidence. First, the shift between the distributions of richness count (see Fig. 3 in LNCG) supports this conclusion, and in particular the respective richness values at which the incompleteness sets in. Second, it is also consistent with the apparent offset in the relation between C_{ACO} and C_{EDCC} (see Fig. 6 in LNCG). The 'offset' between the two richness counts is probably largely due to different methods used in correcting for the field. Third, the very large spread in the relation between the two richness counts, the reason for which is not so obvious, results in about one-third of the ACO clusters with $C_{ACO} \geq 50$ having a count $C_{EDCC} < 30$. Conversely, about one-third of the clusters in the ACO catalogue for which LNCG obtained a count of more than 30 does not meet the $R_{ACO} \geq 1$ criterion (i.e. has $C_{ACO} < 50$).

One can now try to estimate how many clusters with $R_{ACO} \geq 1$ in our volume have been missed by ACO. Note that the complementary question, namely how many clusters in the ACO catalogue with $R_{ACO} \geq 1$ and $m_{10} \leq 16.9$ do not exist according to LNCG, is not relevant for the present argument, as such ACO cluster candidates will have been shown by spectroscopy to be non-existent (there are probably one or two examples in the ENACS). As to the first question we find, from Fig. 10 in LNCG that of the clusters in the EDCC without a counterpart in the ACO catalogue, only 5 have $m_{10}(b_J) \leq 17.7$ (which corresponds to $m_{10}(V) \leq 16.9$) *as well as* a richness count $C_{EDCC} \geq 30$ (which we assume to correspond to $C_{ACO} \geq 50$). Note that the EDCC is at high galactic latitude (with $b \lesssim -45°$), so that Galactic obscuration does not play a rôle in this comparison.

Among these 5 clusters, there are two for which the richness is uncertain, but unlikely to be less than 30. We therefore conclude that these 5 clusters are most likely true $R \geq 1$ clusters that were missed by ACO (for whatever reason). Two of these 5 clusters have $m_{10}(b_J) \leq 17.1$ while the others have $m_{10}(b_J) > 17.3$. We assume therefore that 2 clusters with $z \lesssim 0.08$ have been missed in the solid angle of the EDCC by Abell et al. (1989), and that the other 3 clusters missed have $0.08 \lesssim z \leq 0.1$. As the solid angle of our sample is 5.1 times larger than that of the EDCC, we estimate that from our sample 10 $R_{ACO} \geq 1$ clusters with $z \lesssim 0.08$, and 15 $R_{ACO} \geq 1$ clusters with $0.08 \lesssim z \leq 0.1$ are missing.

At first sight it might seem that these numbers should be reduced by one-third, because of the fact that only two-thirds of the $C_{EDCC} \geq 30$ clusters have $C_{ACO} \geq 50$. However, that would ignore the fact that among the clusters with $C_{EDCC} < 30$, a certain fraction has $C_{ACO} \geq 50$, of which a few are also likely to have been missed by Abell et al. (1989). On the other hand, we consider these estimates of the number of clusters missing from our sample as upper limits, for the following reason. Near the richness completeness limit of a cluster sample there is some arbitrariness in accepting and rejecting clusters due to the uncertainties in the richness estimates. Because the number of clusters increases with decreasing C_{ACO}, it is likely that we have accepted slightly more clusters than we should have done, as a result of the noise in the C_{ACO} estimates.

From these arguments we estimate the true number of $C_{ACO} \geq 50$ clusters in the near half of the volume to be between 74 and 84, or 79 ± 5 (which then implies a total number of 158 $\pm$ 10 such clusters out to $z = 0.1$ assuming a constant space density). The 79 ± 5 $C_{ACO} \geq 50$ clusters represent a space density of $8.6 \pm 0.6 \times 10^{-6}\, h^3$ Mpc^{-3}. This is slightly higher than most previous estimates of the density of $R_{ACO} \geq 1$ clusters (e.g. by Bahcall & Soneira 1983, Postman et al. 1992, Peacock & West 1992, and Zabludoff et al. 1993, hereafter ZGHR). The difference with other work is largely due to our correction of the intrinsic incompleteness of the ACO catalogue on the basis of the comparison with the EDCC. Note that our value is quite

© European Southern Observatory • Provided by the NASA Astrophysics Data System

1996A&A...310...31M

a bit lower than that obtained by Scaramella et al. (1991) for the Southern ACO clusters. These authors found a density of $12.5 \times 10^{-6}\, h^3$ Mpc^{-3}, which does not seem to be consistent with our data.

In the determination of the distribution of velocity dispersions for the $R_{\rm ACO} \geq 1$ clusters (in Sect. 6), we will assume that the incompleteness of the $R_{\rm ACO} \geq 1$ sample can be corrected for simply by adjusting the density of clusters by the factor 158/80 (as we have velocity dispersions for only 80 out of an implied total of 158 clusters). This means that we will assume that the incompleteness only affects the number of clusters, and that our estimate of the σ_V distribution for $0.08 \lesssim z \leq 0.1$ is not biased with respect to that found for $z \lesssim 0.08$.

Our assumption that the total number of $R_{\rm ACO} \geq 1$ clusters is 158 ± 10 immediately implies that we have missed between 20 and 30 clusters in the outer half of our volume. It is not easy to account for this number unambiguously from first principles. However, the number does not seem implausible. Earlier, we estimated from a comparison with the EDCC that between 10 and 20 clusters have probably been missed by Abell et al. (1989) in the outer half of the volume (for whatever reason). This leaves between about 10 and 20 clusters to be accounted for by two effects: namely the m_{10} limit that we imposed in the definition of the sample, and the effects of Galactic obscuration.

Galactic obscuration may indeed have caused some clusters at low latitudes and close to the redshift limit to have been left out of the sample. Note, however, that Peacock & West (1992) argue quite convincingly that the effects of Galactic obscuration do not operate below $z \approx 0.08$, a conclusion that seems well supported by the data in Fig. 3. For $R \geq 1$ clusters at latitudes $|b| \geq 30°$ and with distance class $D \leq 4$ (i.e. $m_{10} \lesssim 16.4$) Bahcall & Soneira (1983) and Postman et al. (1992) propose a cluster selection function varying with galactic latitude as

$$P(b) = 10^{0.32(1-\csc|b|)}.$$

This function also seems to give an acceptable description for Southern clusters with distance class 5 and 6, and is supposed to be largely caused by the effects of Galactic obscuration. For our sample, this would imply that we have missed about 13% of the estimated total of 158, or about 21 clusters, as a result of Galactic obscuration. In the light of the result of Peacock & West (1992), as well as the data in Fig. 3, all these missing clusters must have $z \gtrsim 0.08$.

Within the uncertainties, our interpretation of the observed redshift distribution of $R_{\rm ACO} \geq 1$ clusters thus seems to be consistent with all available information.

4.2. The sample of 33 clusters with $C_{\rm 3D} \geq 75$ and $N \geq 10$

In Sect. 3 we argued, on the basis of the data in Fig. 1c, that our cluster sample with $C_{\rm ACO} \geq 50$ probably is an acceptable substitute for a complete sample with $C_{\rm 3D} \geq 50$. The reason for this is that the two richness values scatter around the $C_{\rm ACO} = C_{\rm 3D}$-line, while the scatter (even though it is appreciable) appears quite symmetric around this line. From the same figure it is also clear that it is not practically feasible to construct a sample complete down $C_{\rm 3D} = 50$ on the basis of the ACO catalogue. That would require the ACO catalogue to be complete down to $C_{\rm ACO} \approx 20$, given the width of the $f_{\rm main}$ distribution.

However, the data in Fig. 1c also show that from our $C_{\rm ACO} \geq 50$ complete sample it is possible to construct a subsample that is complete with respect to intrinsic richness for $C_{\rm 3D} \geq 75$. In Table 1a there are 34 clusters with $C_{3D} \geq 75$, for one of which no velocity dispersion could be determined. In addition, there are 33 clusters in Table 1a that have $C_{\rm ACO} + C_{\rm bck} > 75.0$ but for which $f_{\rm main}$ is not available. Using the distribution of $f_{\rm main}$ given in Fig. 1a, we estimate that 10.2 of these would turn out to have $C_{\rm 3D} \geq 75$ if we measured their $f_{\rm main}$. This brings the estimated total number of clusters with $C_{\rm 3D} \geq 75$ in Table 1a to 44.2.

Finally, one must add an estimated contribution to this sample of $C_{\rm 3D} \gtrsim 75$ clusters that have probably been missed by Abell et al. (1989). As before, the comparison between ACO and EDCC allows us to estimate this contribution. In principle, one would want to estimate the number of clusters missed with $C_{\rm 3D} \geq 75$. As the richnesses of 2 of the 5 clusters missed by ACO in the solid angle of the EDCC are uncertain, this cannot be done. Therefore, we will assume that the distribution over richness of the 5 clusters missed is the same as that of all clusters in our sample. Hence, as 44.2 of the 128 clusters with $C_{\rm ACO}$ have $C_{\rm 3D} \geq 75$, we estimate that 1.8 of the 5 missing clusters have $C_{\rm 3D} \geq 75$. Taking into account the ratio of the solid angles (see Sect. 4.1) this implies that 9.2 clusters with $C_{\rm 3D} \geq 75$ have been missed by ACO in our 'cone' volume. This brings the estimated total number of such clusters in the 'cone' to 53.4 ± 5, which represents a density of $2.9 \pm 0.3 \times 10^{-6}\, h^3$ Mpc^{-3}.

4.3. Some remarks on the quality of the ACO catalogue

Since serious doubts have been raised over the completeness and reliability of the ACO catalogue, it may be useful to summarize here our findings about its quality.

As was shown in Paper I, the redshift data from the ENACS show that almost all $R_{\rm ACO} \geq 1$ cluster candidates with $m_{10}(V) \leq 16.9$ and $b \leq -30°$ correspond to real systems that are compact in redshift space. In only about 10% of the cases an $R_{\rm ACO} \geq 1$ cluster candidate appears to be the result of a superposition of two almost equally rich (but relatively poorer) systems.

Comparison between the EDCC and ACO catalogues shows that at most ≈15% (i.e. 25/158) of the $C_{\rm EDCC} \geq 30$ clusters (which are expected to have $C_{\rm ACO} \geq 50$) with $m_{10}(V) \leq 16.9$ in the EDCC do not appear in the ACO catalogue. From this, one can conclude that *the ACO catalogue is at least 85% complete* for $R_{\rm ACO} \geq 1$ clusters out to a redshift $z \approx 0.1$ (see also Briel & Henry 1993). Out to $z = 0.08$ the completeness is even higher, viz. 94%. If one takes into account the effects of Galactic obscuration the overall completeness of the ACO catalogue for $|b| \geq 30°$ apparently decreases to about 80% (viz. 128/158).

On average, about three quarters of the galaxies in the direction of $R_{\rm ACO} \geq 1$ clusters with $z \lesssim 0.1$ are in the main system, i.e. the effect of fore- and background contamination

© European Southern Observatory • Provided by the NASA Astrophysics Data System

1996A&A...310...31M

is substantial. However, if one takes into account the effect of field contamination by deriving C_{3D}, the intrinsic 3-D richness of the clusters, it appears that the field-corrected ACO richness is statistically equivalent to the intrinsic richness. This means that one can use a complete sample of clusters with $C_{ACO} \geq 50$ to investigate the statistical properties of a sample of clusters complete down to $C_{3D} \approx 50$. The relation between C_{ACO} and C_{3D} however shows a large spread; as a result it is not possible to select from the $C_{ACO} \geq 50$ cluster sample a subsample that is complete with respect to C_{3D} for values of C_{3D} less than about 75.

We have thus demonstrated that our sample of 128 clusters in the ACO catalogue with $C_{ACO} \geq 50$ and $z \leq 0.1$ can be used as a statistical sample for the study of the properties of clusters of galaxies. The subsample of 33 clusters with $C_{3D} \geq 75$ and $N \geq 10$ is truly complete with respect to C_{3D} and can therefore be used to check the results from the larger sample.

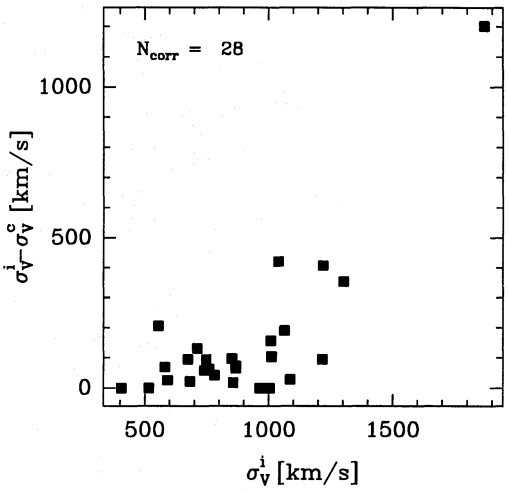

Fig. 4. The decrease in velocity dispersion as a result of the removal of interlopers, versus the initial, uncorrected value of the velocity dispersion.

5. The estimation of the velocity dispersions

For a determination of the distribution of cluster velocity dispersions, one must address several points. First, it is very important that the individual estimates of the global velocity dispersions are as unbiased as possible, as any bias may systematically alter the shape and amplitude of the distribution. For example, when we identified the systems in velocity space using a fixed velocity gap, we did not discuss the plausibility of membership of individual galaxies. Before calculating the global velocity dispersion we must take special care to remove fore- and background galaxies that cannot be members of the system on physical grounds. Leaving such non-members in the system will in general lead to an overestimation of the global velocity dispersion. Secondly, it has been shown that the velocity dispersion may vary with position in the cluster, so that the global velocity dispersion can depend on the size of the aperture within which it is calculated. Finally, radial velocities are generally measured only for a bright subset of the galaxy population. If luminosity segregation is present this will generally cause the velocity dispersion to be underestimated.

5.1. The removal of interloper galaxies

It is well-known that in determining velocity dispersions one has to be very careful not to overestimate σ_V as a result of the presence of non-members or 'outliers'. Recently, den Hartog & Katgert (1995) have shown that velocity dispersions will be overestimated due to the presence of 'interlopers', i.e. due to galaxies that have 'survived' the 1000 km/s fixed-gap criterion for membership, but that are nevertheless unlikely to be members of the cluster. For the removal of such interlopers, these authors developed an iterative procedure that employs the combined positional and velocity information to identify galaxies that are probably not cluster members.

The procedure starts by estimating a mass profile from an application of the virial theorem to galaxies in concentric (cylindrical) cross-sections through the cluster with varying radii. Subsequently, for each individual galaxy one investigates whether the observed line-of-sight velocity is consistent with the galaxy being on a radial orbit with a velocity less than the escape velocity, or on a bound circular orbit. If the observed velocity is inconsistent with either of these extreme assumptions about the shape of the orbit, the galaxy is flagged as an interloper (i.e. a non-member), and not used in the computation of the mass profile in the next iteration step. This procedure is repeated until the number of member galaxies becomes stable, which usually happens after only a few iteration steps.

In order to ensure that the definition of an interloper and the value of the cluster velocity dispersion is independent of the redshift of the cluster, it is necessary to convert the velocities of galaxies with respect to the cluster to the rest frame of the cluster (e.g. Danese et al. 1980). Because the elimination of interlopers changes the estimated average cluster redshift (but only slightly) this correction is applied to the original data in each iteration step.

The procedure has been tested on the set of 75 model clusters presented by Van Kampen (1994). This set of model clusters is designed to mimic a sample complete with respect to total mass in a volume that is comparable to that of our $z \leq 0.1$ sample. The initial conditions were generated for an $\Omega = 1$ CDM scenario. Individual cluster models have reasonable mass resolution and contain dark matter particles as well as soft galaxy particles that are formed according to a prescription that involves percolation and a virial condition. A typical simulation has a volume of about $(30h^{-1}$ Mpc$)^3$ and contains $O(10^5)$ particles. In these models the membership of galaxies follows unequivocally from the position with respect to the turn-around radius. It appears that the interloper removal works very well: in the central region (i.e. within the Abell radius) 90% of the non-members are indeed removed, and those that are not removed have a velocity dispersion that is essentialy equal to that of the member galax-

© European Southern Observatory • Provided by the NASA Astrophysics Data System

1996A&A...310...31M

ies. In the same region only 0.4% of the cluster members is inadvertently removed.

Because the procedure by which we removed interlopers requires a reliable position for the cluster centre and a reasonably well-determined mass profile, we have applied it only to the 28 clusters for which at least 50 redshifts are available. This means that the density of systems with the largest velocity dispersions may still be somewhat overestimated, as some of the largest dispersions are for systems with less than 50 redshifts. As a result the dispersion distribution could in reality fall off even slightly steeper towards high dispersions at the high end than it appears to do. However, for the clusters with less than 50 redshifts we have used the robust biweight estimator for the velocity dispersion (see Beers et al. 1990), so that the influence of unremoved interlopers in the tails of the velocity distribution is strongly reduced.

We have used as many redshifts as possible for each cluster. In 5 cases (i.e. for A0119, A0151, A2717, A3128, A3667) we have combined existing data from the literature with the new redshifts obtained in the ENACS. Before combining the two sets of data we have investigated the consistency of the two redshift scales. The comparison is made for galaxies of which the position is the same in both surveys to within 20″. The redshift scales generally agree to within the uncertainties (see also Table 2 in Paper I).

In Fig. 4 we show, for the 28 systems with at least 50 members, the decrease of the global velocity dispersion as a function of the value of the dispersion before the interlopers were removed. For dispersions below about 900 km/s the reduction is at most about 10%. It is clear that the decrease can be much larger for the largest dispersions, with reductions of as much as 25 to 30%. The point near the upper right-hand corner refers to A151, before and after the separation of the 2 low redshift systems. In two clusters, A85 and A3151, the interloper removal failed to delete a group of interlopers. In the wedge diagrams the two groups were clearly compact in velocity and spatial extent, with a velocity offset of $\approx$ 2000 km/s with respect to the main system. We have removed these groups by hand.

Our analysis indicates that systems with global velocity dispersions larger than 1200 km/s have such low space density (if they exist at all) that in our volume they do not occur. This would seem to be at variance with the result of ZGHR, who find one cluster, A2152, with a dispersion of 1346 km/s in a sample of 25 clusters, in a volume that is about a factor of 5 smaller than ours. However, it must be said that, had the cluster A2152 appeared in our sample (with the same number of redshifts that ZGHR had available, viz. 21), we would probably also have found a high velocity dispersion. However, had 50 redshifts been available, we would almost certainly have eliminated quite a few interlopers, and would thereby probably have reduced the dispersion substantially. Therefore, a distribution of velocity dispersions becomes less biased towards high dispersion values, when the average number of redshifts per cluster increases.

The absence of systems with very large velocity dispersions in our sample is due to the large fraction of systems for which we could eliminate non-members using a physical criterion. As we have discussed extensively in Paper I, it is very unlikely that the absence of very large velocity dispersions in our sample is due to the method by which we defined the systems in the first place. If we had used the method of ZGHR to define the systems (see Table 6 in Paper I for detailed information) one or two systems which we have broken up would have remained single. However, when we identify our clusters with the ZGHR method and subsequently remove the interlopers, we find essentially the same clusters with the same velocity dispersions. It thus appears that quite a few of the galaxies in the clusters for which ZGHR find a very large velocity dispersion are unlikely to be members of the system.

5.2. The effects of aperture variations and luminosity segregation

Another possible bias in estimating velocity dispersions is due to the fact that the velocity dispersion frequently varies significantly with distance from the cluster centre (see e.g. den Hartog and Katgert, 1995). Differences in the physical size of the aperture within which the velocities are measured are inevitable for a sample of clusters with redshifts between 0.02 and 0.1. However, the sizes of the apertures used in the observations have a dispersion of only about 30% around the average value of about 0.9 h^{-1} Mpc . On the basis of the velocity dispersion profiles discussed by den Hartog and Katgert (ibid.) and in agreement with Girardi et al. (1993) we estimate that corrections for variations in the aperture in practice are at most about 10% (and can be both positive and negative). They are thus substantially smaller than the largest corrections applied to the dispersions due to interloper removal (which are exclusively negative). We have decided not to attempt to apply corrections for aperture variations based on an average velocity dispersion profile, as this will only introduce noise and is not expected to change the results in a systematic way.

den Hartog and Katgert (ibid.) found signs of luminosity segregation in approximately 20% of the clusters in their sample. Hence, it is necessary to check that our velocity dispersions are not biased in a systematic way as a result of the fact that we have sampled for many clusters only the brightest galaxies in the central regions of the clusters. Luminosity segregation is a manifestation of the physical processes of mass segregation (heavy galaxies move slower and their distribution is more centrally concentrated than that of light galaxies) and velocity bias (the velocity dispersion of the galaxies is lower than that of the dark matter particles). The reality of mass segregation and velocity bias is still a matter of dispute (see e.g. Carlberg 1994, versus e.g. Katz et al. 1992, Biviano et al. 1992, Lubin & Bahcall 1993, and Van Kampen 1995). Moreover, significant mass segregation may not be readily observable if it is accompanied by significant variations in $\mathcal{M}/\mathcal{L}$–ratio .

We have tested for the presence of luminosity segregation in our cluster sample, and will discuss the results in a forthcoming paper. It appears that luminosity segregation exists, but that it is exclusively linked to the very brightest cluster galaxies, which appear to move very much slower than the other galaxies.

© European Southern Observatory • Provided by the NASA Astrophysics Data System

1996A&A...310...31M

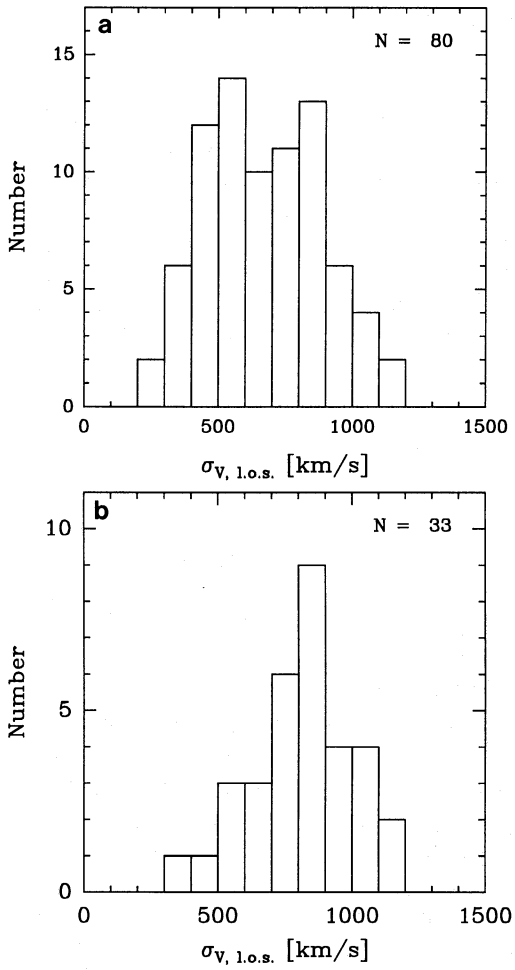

Fig. 5. The apparent distribution of cluster velocity dispersions, (**a**) for the sample of 80 clusters with $C_{\rm ACO} \geq 50$ and $z \leq 0.1$; (**b**) for the subsample of 33 clusters with $C_{\rm 3D} \geq 75$.

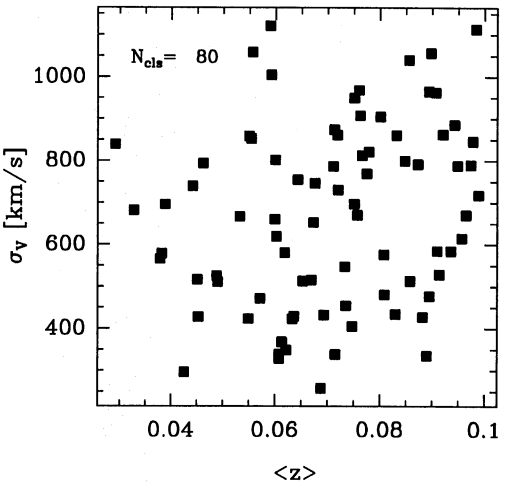

Fig. 6. Distribution with respect to redshift and velocity dispersion of the 80 systems with $C_{\rm ACO} \geq 50$ and $z \leq 0.1$.

As our velocity dispersions are based on at least 10 (but often many more) redshifts, the effect of luminosity segregation is completely negligible in the context of the present discussion.

6. The distribution of velocity dispersions

By virtue of the significant (but very broad) correlation between richness and velocity dispersion, the largest velocity dispersions are in general found in the systems with the highest richnesses, whereas the low dispersions are found preferentially in the poorer systems. As a result, any sample of clusters presently available is biased against low velocity dispersions, because of the lower limit in richness that defines the sample. This means that any observed (and predicted!) distribution of cluster velocity dispersions refers to a specific richness limit. As a matter of fact, the distribution will in principle be biased for velocity dispersions smaller than the largest value found at the richness limit; above the latter value the distribution is unbiased.

Our estimates of the apparent distributions of σ_V are shown in Figs. 5a and b. They refer to the two subsets of clusters: viz. the complete sample of 80 clusters with $z \leq 0.1$ and $C_{\rm ACO} \geq 50$ and the complete subsample of 33 clusters with $C_{\rm 3D} \geq 75$. As we discussed before, the latter is truly complete with respect to intrinsic 3-D richness (i.e. fore- and background contamination has been taken into account) and the completeness with respect to redshift is beyond suspicion. We also found that the sample of 80 $C_{\rm ACO} \geq 50$ clusters can be used as a substitute for a $C_{\rm 3D} \geq 50$ sample. However, as it is somewhat incomplete near the redshift limit we can derive an unbiased estimate of the σ_V distribution only if there is no systematic change in our sample of σ_V with redshift.

In Fig. 6 we show that there is indeed no evidence for a significant correlation of velocity dispersion with redshift in our sample. The lack of systems with $\sigma_V \gtrsim 900$ km/s below a redshift of about 0.05 is not considered significant in view of the small volume sampled. It is also encouraging that there is no clear bias against systems with low values of σ_V, between $z = 0.08$ and $z = 0.1$. Therefore, the data in Fig. 6 indicate that the result for the sample of 80 systems with $z \leq 0.1$ and with $C_{\rm ACO} \geq 50$ should be equally reliable as that for the subsample of 33 $C_{\rm 3D} \geq 75$ systems, with the advantage of larger statistical weight.

In Fig. 7 we show the cumulative distribution of σ_V for the sample of 80 clusters with $C_{\rm ACO} \geq 50$ (full-drawn line) and for the subsample of 33 clusters with $C_{\rm 3D} \geq 75$ (dashed line). Note that the densities follow directly from the space densities that we derived in Sects. 4.1 and 4.2, and have thus not been scaled to some external cluster density (as is sometimes done in the literature). For comparison, and to illustrate the effect of the interloper removal, we also show the cumulative distribution of σ_V for the 80 cluster sample, when no interlopers are removed, i.e with σ_V for the clusters with 50 redshifts or more determined only with the robust biweight estimator (dotted line). It is clear that without interloper removal the distribution of σ_V is significantly biased for $\sigma_V \gtrsim 800$ km/s.

© European Southern Observatory • Provided by the NASA Astrophysics Data System

1996A&A...310...31M

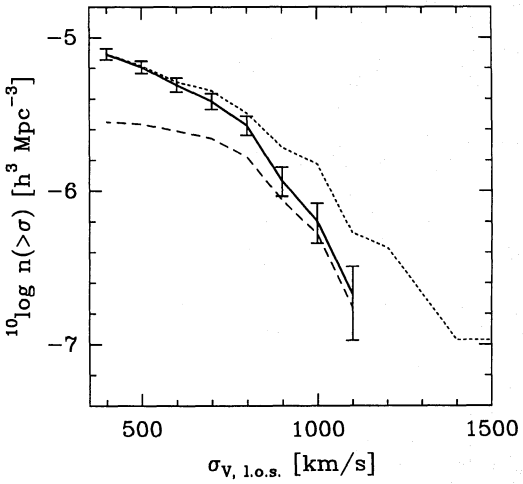

Fig. 7. The cumulative distribution of cluster velocity dispersions. Solid line: for the sample of 80 clusters with $C_{\rm ACO} \geq 50$ and $z \leq 0.1$. Dotted line: for the sample of 80 clusters with $C_{\rm ACO} \geq 50$ and $z \leq 0.1$, but without interlopers removed. Dashed line: for the sample of 33 clusters with $C_{\rm 3D} \geq 75$ and $z \leq 0.1$.

The (interloper-corrected) distributions for the two samples agree very well for $\sigma_V \gtrsim 900$ km/s. This is not surprising because, as we will see below, there are hardly any clusters with $\sigma_V \geq 900$ km/s that have $C_{\rm 3D} < 75$. The good agreement therefore just shows that the ratio of the space densities derived in Sects. 4.1 and 4.2 is quite good. The two distributions also illustrate the bias against low values of σ_V. The value of σ_V at which the bias sets in and the magnitude of the bias are seen to depend on the richness completeness limit of the sample in a way that is consistent with the discussion at the beginning of this section. For the sample with $C_{\rm 3D} \geq 75$ the incompleteness starts at $\sigma_V \approx 900$ km/s, while for the sample with $C_{\rm ACO} \geq 50$ it starts at $\sigma_V \approx 800$ km/s.

For $\sigma_V \geq 800$ km/s the cumulative distribution for the sample of 80 clusters can be parametrized as follows:

$$\log n(>\sigma_V) = -5.6 - 0.0036(\sigma_V - 800\,\mathrm{km/s}) \quad h^3\ \mathrm{Mpc}^{-3}$$

For $\sigma_V < 800$ km/s the same distribution also seems to be described fairly accurately by a power law, but the significance of that fit is much less apparent because of the bias that is likely to increase with decreasing σ_V.

ZGHR have tried to correct the bias against low-velocity dispersion systems by combining clusters and dense groups. Indeed, it appears that continuation of the above power law fit down to $\sigma_V = 700$ km/s would predict, within the errors, the correct density $n(>700\,\mathrm{km/s})$ for the combination of clusters and dense groups. However, as the definition and selection of dense groups is different from that of rich clusters, it is not unlikely that the intrinsic properties of the groups, such as σ_V, as well as their spatial density may differ systematically from that of the clusters. Also, for the dense groups a similar bias operates as for the clusters. Combination of the two σ_V distributions is therefore not without problems.

It is of some interest to have a closer look at the values of σ_V below which the two distributions are biased as a result of the lower limits in $C_{\rm ACO}$ and $C_{\rm 3D}$ that define the samples. These values of σ_V are the maximum values found near the cut-off in richness, and they can be estimated from Fig. 8, in which we show several distributions of σ_V against richness. From the distribution of σ_V against $C_{\rm ACO}$, shown in Fig. 8a, it appears that the maximum σ_V near the richness limit $C_{\rm ACO} = 50$ is about 800 km/s.

In Fig. 8b we show σ_V vs. richness for the subset of ENACS clusters for which either LNCG (squares) or Dalton (priv. comm.; diamonds) give an alternative, machine-based estimate of the richness. In Fig. 8b the ordinate is $C_{\rm EDCC}$+20 rather than $C_{\rm EDCC}$, because there seems to be a systematic offset between $C_{\rm ACO}$ and $C_{\rm EDCC}$ of about 20 (see Sect. 4.1). It is clear that for a richness limit of 50 in the machine-based counts, the bias is again absent only for $\sigma_V \gtrsim 800$ km/s.

In Fig. 8c we show velocity dispersion vs. richness count $C_{\rm APM}$ from the APM cluster catalogue, for the 37 clusters in the APM catalogue of which the positions coincide with that of a cluster in our sample to within half an Abell radius. Note that Dalton et al. (1994) have calculated the richness inside half an Abell radius and within a variable magnitude interval based on the luminosity function in the region of the cluster, in order to be less sensitive to interlopers. As a result $C_{\rm APM}$ is systematically lower than $C_{\rm ACO}$, and the richness limit $C_{\rm ACO} = 50$ corresponds to $C_{\rm APM} = 35$ (Efstathiou et al. 1992a). From Fig. 8c we conclude that the bias against low velocity dispersions sets in at $\sigma_V \approx 800$ km/s.

From the fact that the three left-hand panels in Fig. 8 are qualitatively very similar we conclude that the large spread in Fig. 8a is not primarily due to errors in the values of $C_{\rm ACO}$, as a similar spread is seen for the two other catalogues. Therefore, we conclude that the large spread in velocity dispersion for a fixed value of 2-D richness is probably (at least partially) intrinsic to the clusters.

In Fig. 8d we show the relation between σ_V and $C_{\rm 3D}$, with the latter based on $C_{\rm ACO}$. It appears that the relation is less broad than that in Fig. 8a. Apparently, the correction for superposition effects (which we could only apply thanks to the redshift information) results in a fairly significant decrease of the spread in the relation. In Fig. 8d the existence of an upper limit to the velocity dispersion of ≈900 km/s at the richness limit of 75 is very clearly illustrated. The spread in the relation between σ_V and $C_{\rm 3D}$ in Fig. 8d is probably not primarily due to errors in the values $C_{\rm ACO}$. This is supported by the data in Figs. 8e and 8f, where we show the relation between σ_V and machine-based counts that have been corrected for superposition effects.

We conclude therefore that the scatter between σ_V and richness (in whichever way it is measured) must largely be intrinsic. In other words: a given velocity dispersion may be found in clusters of quite different richnesses, while clusters of a given richness span a large range of velocity dispersion.

© European Southern Observatory • Provided by the NASA Astrophysics Data System

1996A&A...310...31M

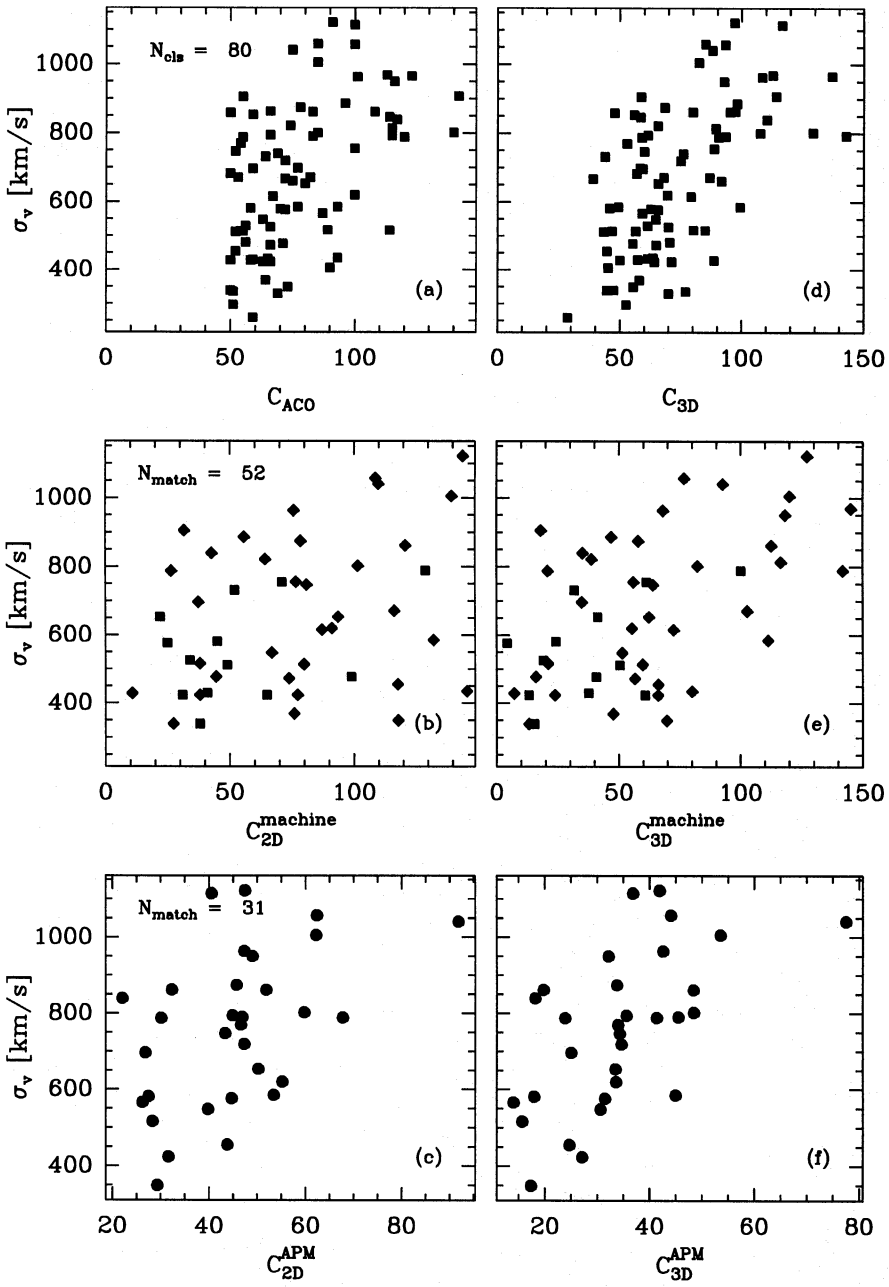

Fig. 8a–f. Velocity dispersion σ_V versus richness. (**a**) σ_V vs. $C_{\rm ACO}$ for all main systems in the ENACS sample. (**b**) σ_V vs. $C_{\rm EDCC}$ + 20 (squares) and σ_V vs. $C_{\rm 2D}$, obtained by Dalton (1992) from application of the ACO cluster definition to candidate clusters in the APM survey (diamonds). (**c**) σ_V vs. $C_{\rm APM}$, from the APM cluster catalogue listed in Dalton et al. (1994). (**d**) As (**a**), but now for $C_{\rm 3D} = f_{\rm main} \times (C_{\rm ACO} + C_{\rm bck})$, i.e. the intrinsic richness corrected for superposition effects. (**e**) As (**d**), but now for machine-based 'ACO' counts corrected for superposition effects. Note that the EDCC counts were also corrected, viz. $C_{\rm 3D} = f_{\rm main} \times (C_{\rm EDCC} + n_{\rm bck})$, where $n_{\rm bck}$ is the number of background galaxies estimated by LNCG. (**f**) As (**d**) but now for the APM clusters, corrected for superposition effects.

7. Discussion

In the following we will make two types of comparison of the results obtained here with earlier results. First we will compare with other determinations of the cumulative distribution of cluster velocity dispersions $n(>\sigma_V)$, as well as with the distributions of cluster X-ray temperatures $n(>T_X)$. Subsequently, we will discuss the relation between our result and some model predictions for $n(>\sigma_V)$ from the literature.

7.1. Comparison with other data

There are several other determinations of $n(>\sigma_V)$ in the literature. Recent papers on the subject are e.g. those by Girardi et al. (1993), and by ZGHR. The result of Girardi et al. (1993) is based on a compilation of redshifts for cluster galaxies. As a result, the amplitude of $n(>\sigma_V)$ is not known in absolute terms, but has been inferred from the integrated fraction of clusters together with an external estimate of the total density of rich clusters. Collins et al. (1995) also present a distribution of σ_V that is not normalized. On the contrary, ZHGR present, like we do, an estimate of $n(>\sigma_V)$ with a calibrated space density. A comparison with the results of Girardi et al. (1993) and ZGHR is given in Fig. 9a, where the result of Girardi et al. (1993) has been scaled to the density of rich clusters derived in Sect. 4.1, rather than that given by Bahcall and Soneira (1983).

Although the previous estimates of $n(>\sigma_V)$ involved clipping of 'outliers', none employed the removal of interlopers as described in Sect. 5.1 , and therefore it is not too surprising

© European Southern Observatory • Provided by the NASA Astrophysics Data System

1996A&A...310...31M

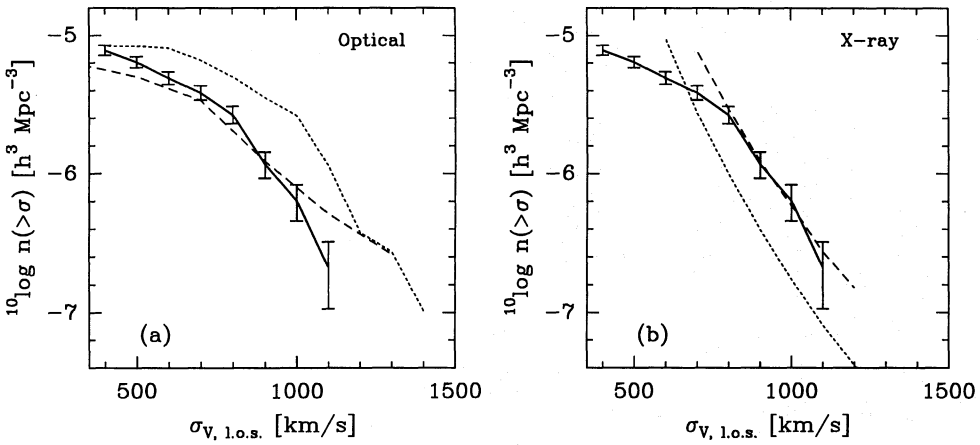

Fig. 9a and b. Comparison of the present cumulative distributions of velocity dispersions with distributions from the literature. The solid line in both figures refers to our sample of 80 clusters with $z \leq 0.1$. (**a**) Optical data: Girardi et al. (1993, dotted line), ZGHR (short dashed line). (**b**) X-ray data: Henry & Arnaud (1991, dashed line) and Edge et al. (1990, dotted line).

that for $\sigma_V \gtrsim 900$ km/s our result is systematically lower than the other two. Girardi et al. (1993) obtain a similar slope but a (perhaps not very certain) amplitude that is at least two times higher than ours. We do not show the result of Collins et al. separately as it appears to agree with that of Girardi et al. On the other hand, the result of ZGHR agrees very nicely with ours for $\sigma_V \lesssim 900$ km/s, but for larger values of σ_V they obtain a slope that is definitely less steep than ours.

Our upper limit on the occurence of clusters with $\sigma_V \gtrsim 1200$ km/s is much more severe than any previous result based on optical data, namely that the space density of such clusters is less than one in our survey volume of $1.8 \times 10^7\ h^{-3}$Mpc^3. As we discussed above, this is almost entirely due to our removal from the redshift data of those interlopers that can only be recognized on the basis of the combination of radial velocity *and* projected position within the cluster.

In Fig. 9b we compare our result with distributions of the cluster X-ray temperature T_X by Henry & Arnaud (1991) and by Edge et al. (1990). In transforming the T_X scale into a σ_V scale we assumed that $\sigma_V^2 = (kT_X/\mu m_H)$, where μ and m_H have their usual meaning. The reason for the discrepancy between the two X-ray results is not known. ZGHR have suggested that the discrepancy is due to differences in normalization caused by different fitting procedures, sample size and sample completeness. The agreement between our result and that of Henry & Arnaud (1991) is excellent for $\sigma_V \gtrsim 800$ km/s. Both the amplitude and the slope agree very well, and to us this suggests that the removal of interlopers is necessary, and that our removal procedure is adequate. It also suggests that the velocity dispersions in excess of 1200 km/s, found by others, must indeed almost all be overestimates caused by interlopers. Interestingly, the two results start to diverge below ≈800 km/s. Although one cannot claim that $n(> T_X)$ is very well determined in that range there is at least no contradiction with the conclusion that we reached in Sect. 6, namely that our $n(> \sigma_V)$ must start to become underestimated below ≈800 km/s as a result of the richness limit of our cluster sample.

The extremely good agreement between our $n(> \sigma_V)$ and the $n(> T_X)$ by Henry & Arnaud (1991) for $\sigma_V \gtrsim 800$ km/s, for an assumed value of $\beta = \sigma_V^2/(kT_X/\mu m_H) = 1$ strongly suggests that X-ray temperatures and velocity dispersions statistically measure the same cluster property. This is in agreement with earlier results of Lubin & Bahcall (1993), Gerbal et al. (1994), and den Hartog & Katgert (1995) who also find that it is not necessary that the ratio of 'dynamical' and X-ray temperatures differs from 1.0. Of course, in our case this statement only refers to the *sample* of clusters, and it has not been proven to be valid for individual clusters. On the basis of the data in Fig. 9b we conclude that the *average* value of β must lie between 0.7 (the value required if the upper range of our $n(> \sigma_V)$ determinations must coincide with the result of Edge et al. 1990), and 1.1 (the value required if the lower range of our data must coincide with the result of Henry & Arnaud 1991).

7.2. Requirements for useful comparison with models

There are quite a few papers in the literature in which model calculations of clusters of galaxies are presented from which one can, in principle, derive model predictions of $n(> \sigma_V)$. These models are generally of two kinds. First, there are numerical (or analytical) models of a sufficiently large cosmological volume, containing a sample of clusters, each of which is modeled with relatively low resolution. In this case one can obtain a direct estimate of $n(> \sigma_V)$, the normalization of which is unambiguous. A good example of this type of model was described by FWED. Secondly, sets of higher-resolution cluster simulations may be created for which the global properties are distributed as predicted for an arbitrarily chosen, large cosmological volume. In this case, the normalization of $n(> \sigma_V)$ depends on the details of the selection of the set of cluster models. An example of the latter has been described by Van Kampen (1994). Of course, in both cases, the resulting predictions are valid only for the chosen scenario of large-scale structure formation. We will limit ourselves here to a brief discussion of various aspects of the comparison between observations and models, and demonstrate the use of our result in a comparison with the models of FWED and Van Kampen (1994).

A meaningful comparison between observations and models requires that one derives from the models a prediction of exactly the same quantity as one has observed. As we discussed above, our σ_V estimates refer to a *cylinder* with an average radius of 1.0

© European Southern Observatory • Provided by the NASA Astrophysics Data System

1996A&A...310...31M

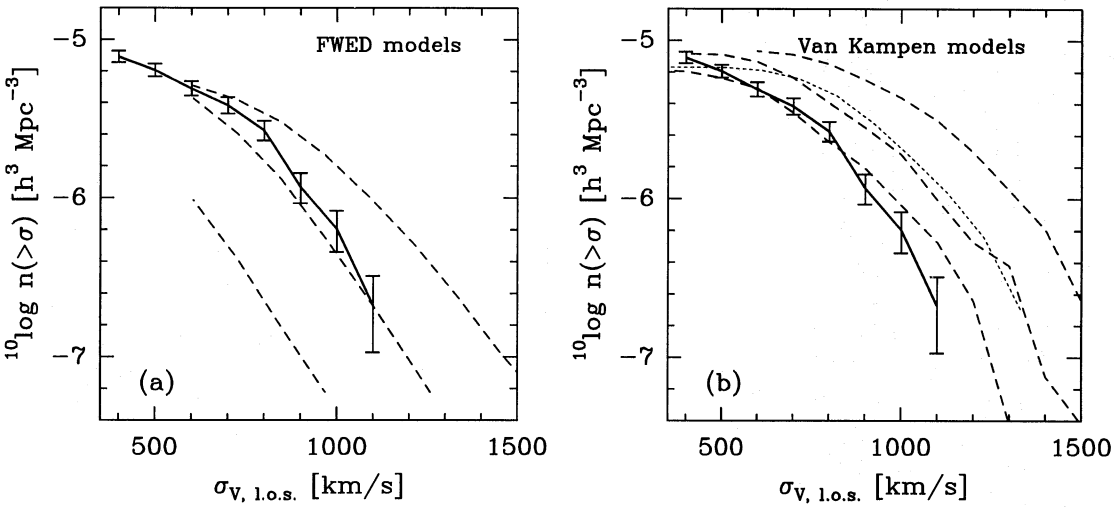

Fig. 10a and b. Comparison of the cumulative distribution of σ_V derived in this paper (solid line) with predictions from standard CDM N-body simulations with different values of the bias parameter b. (**a**) The dashed lines correspond to distributions of the line-of-sight σ_V computed by FWED in *spheres* with radius equal to the Abell radius. These curves were corrected for the aperture effect, the projection effect and the softening effect. The values of b are 2.0, 2.5 and 3.3 (top to bottom). (**b**) Distributions of the line-of-sight σ_V of galaxies in a cylinder with a radius of 1.0 h^{-1} Mpc in Van Kampen's (1994) models. The dashed lines are the distributions for galaxies, for values of b of 1.6, 2.2, and 2.8 (top to bottom). The dotted line gives the distribution of σ_V computed for the dark matter inside a cylinder for $b = 2.2$.

h^{-1} Mpc and a depth of (about) twice the turn-around radius of the cluster. From their models, FWED have calculated the line-of-sight velocity dispersion within a *sphere* with radius equal to the Abell radius. As the latter excludes the, mostly slowly moving, galaxies that are near the turn-around radius, the σ_V values in a sphere are expected to be systematically higher than in a cylinder with the same radius, by as much as 10 %. On the other hand, the value of σ_V also depends on the radius of the cylinder or sphere. On average, σ_V is expected to decrease with increasing radius of the cylinder because, on average, the velocity dispersion tends to decrease with distance from the cluster centre. In a comparison between our data and the model prediction of FWED (who use a sphere with radius 1.5 h^{-1} Mpc as compared to our cylinder with radius 1.0 h^{-1} Mpc) we will assume that the two effects compensate almost exactly. We conclude this from a direct comparison between the two quantities based on the models of Van Kampen (1995). As the models by FWED and Van Kampen use the same $\Omega = 1$ CDM formation scenario, we assume that this conclusion is also valid for the FWED models.

The values of the global σ_V may depend fairly strongly on the details of the integration scheme in the N-body simulations. For instance, the models of FWED do not have much resolution on the scale of galaxies, since huge volumes (of the order of the volume of the ENACS) had to be simulated with $O(2 \cdot 10^5)$ particles. As a result, the scale-length for force softening is well over 100 kpc. Van Kampen (1995) has studied the effect of the softening scale-length on σ_V and finds that for the FWED scale-length the velocity dispersions are 15–20% smaller than for a softening-length of 20 kpc.

Another aspect of the comparison is the identification of the clusters in (particularly) the large-scale simulations. FWED identified 'galaxies', at the end of the simulation, as peaks in the density field, without altering the dynamical properties of the constituent dark particles. First, it is not clear whether galaxies form solely or preferentially from peaks in the initial density field (see e.g. Van de Weygaert & Babul 1994, and Katz et al. 1994). Secondly, Van Kampen (1995) found that the spatial distribution of the 'galaxies' in his models can differ substantially from that of the dark matter. The galaxy identification 'recipe' can thus influence the definition of the clusters and of the cluster sample, as a cluster is identified through the number of galaxies inside an Abell radius.

Finally, it is possible that in clusters the velocity dispersion of the galaxies is 10 – 20% lower than that of the dark matter, as a result of velocity bias (see e.g. Carlberg 1994 and Summers 1993). The reality of velocity bias is still controversial (see e.g. Katz et al. 1992, Lubin & Bahcall 1993 and Van Kampen 1995), and one must be careful to derive the velocity dispersion of the *galaxies* from the models.

7.3. Comparison with selected model predictions

In Fig. 10 we compare our estimate of $n(> \sigma_V)$ to the model predictions from FWED and Van Kampen (1994), which both assume an $\Omega = 1$ CDM formation scenario. In Fig. 10a we compare our result with the predictions by FWED, who identified the $R \geq 1$ clusters in their models as groups of dark and luminous particles for which the luminosity inside a sphere with Abell radius exceeds 42 L^*. We corrected the FWED velocity dispersions for the effects of the fairly large softening parameter by multiplying them by a factor of 1.18. We assumed that the differences related to the use of spherical and cylindrical volumes, as well as different sizes of the aperture, compensate.

© European Southern Observatory • Provided by the NASA Astrophysics Data System

1996A&A...310...31M

For a suitable choice of the bias parameter the observations and predictions can be made to agree fairly well, although one could argue that for $\sigma_V \gtrsim 800$ km/s the slope of the observed $n(>\sigma_V)$ is steeper than that of the predicted $n(>\sigma_V)$ for any bias parameter in the range from 2.0 to 2.5. This may be (partly) due to the fact that FWED convolved their result with assumed errors in σ_V of about 20 %, which is probably a factor of two larger than the errors in our σ_V estimates for $\sigma_V \gtrsim 800$ km/s.

In Fig. 10b we make the comparison with the predictions by Van Kampen (1994), who applied a C_{3D} lower limit for identifying the clusters to be included in the comparison. We have scaled his results to the density of rich clusters derived in Sect. 4.1. For his models we show the distributions of σ_V for the galaxies, but for $b = 2.2$ we also show the distribution for the dark matter; it is clear that the galaxies and dark matter give essentially the same $n(>\sigma_V)$. FWED and Van Kampen (1994) seem to predict different amplitudes of $n(>\sigma_V)$ for the same values of the bias parameter. We do not consider this the proper place to investigate possible explanations for the difference. Suffice it to say that the difference between the cluster identification schemes may well be one of the causes. The observations and predictions can be made to agree fairly well, although one could again argue that for $\sigma_V \gtrsim 800$ km/s the slope of the observed $n(>\sigma_V)$ is significantly steeper than that of the predicted $n(>\sigma_V)$.

From both comparisons we see that for the standard $\Omega = 1$ CDM model a large bias parameter is indicated (between 2.0 and 2.5 for the FWED models and between 2.4 and 2.8 for the models by Van Kampen 1994). For the commonly accepted low value of the bias parameter of about 1.0, the models clearly predict too many clusters with large velocity dispersions. Also, the relative proportions of high- and low-σ_V clusters do not seem to be right.

Our result confirms the conclusions by FWED and White et al. (1993) that the distributions of the velocity dispersions or masses of rich clusters do not support $\Omega = 1$ CDM models with low values of the bias parameter. The high values of the bias parameter, that one infers from the comparisons in Fig. 10, are in conflict with the results for the normalization of the $\Omega = 1$ CDM models on larger scales, from comparisons with e.g. the COBE data (Wright et al. 1992, Efstathiou et al. 1992b), the power spectrum analysis of the QDOT survey (Feldman et al. 1994) and the recent analyses of large-scale streaming (Seljak & Bertschinger 1994).

The important conclusion is therefore that, for $\sigma_V \gtrsim 800$ km/s our observed distribution $n(>\sigma_V)$ provides a very powerful constraint for cosmological scenarios of structure formation. It will not be too long before detailed predictions based on the currently fashionable (or other) alternative scenarios (be it low-density, tilted-spectrum, vacuum-dominated or neutrino-enriched CDM) can be compared, in a proper way, to the observational constraints. Even though it is worthwhile to try and obtain unbiased estimates of $n(>\sigma_V)$ for $\sigma_v \lesssim 800$ km/s, it would seem that the high$-\sigma_V$ tail of the distribution has the largest discriminating power.

8. Summary and conclusions

We have obtained a statistically reliable distribution of velocity dispersions which, for $\sigma_V \gtrsim 800$ km/s, is free from biases and systematic errors, while below 800 km/s it is biased against low values of σ_V in a way that is dictated by the richness limit of our sample, viz. $C_{ACO} \geq 50$.

The observed distribution $n(>\sigma_V)$ offers a reliable constraint for cosmological scenarios, provided model predictions are based on line-of-sight velocity dispersions for all galaxies inside the turn-around radius and inside a projected aperture of $1.0\ h^{-1}$ Mpc , and provided the clusters are selected according to a richness limit that mimics the limit that defines the observed cluster sample.

The sample of ACO clusters with $|b| > 30°$, $C_{ACO} \geq 50$ and $z \leq 0.1$ is ≈85% complete. We find that the density of clusters with an apparent richness $C_{ACO} \geq 50$ is $8.6 \pm 0.6 \times 10^{-6}\ h^3$ Mpc^{-3}, which is slightly higher than earlier determinations (e.g. by Bahcall & Soneira 1983, Peacock and West 1992, and ZGHR). We show that one can define a complete subsample of the $C_{ACO} \geq 50$ sample that contains all clusters with an intrinsic 3-D richness $C_{3D} \geq 75$; the density of the latter is $2.9 \pm 0.3 \times 10^{-6}\ h^3$ Mpc^{-3}.

We find that cluster richness is a bad predictor of the velocity dispersion (whether it is based on ACO or machine counts) due to the very broad correlation between the two cluster properties. It appears that the spread in this correlation must be largely intrinsic, i.e. not due to measurement errors. As a result, all samples of clusters that are selected to be complete with respect to richness are biased against low-σ_V systems.

The space density of clusters with $\sigma_V > 1200$ km/s is less than $0.54 \times 10^{-7}\ h^3$ Mpc^{-3}. This is in accordance with the limits from the space density of hot X-ray clusters. From the good agreement between $n(>\sigma_V)$ and $n(>T_X)$ we conclude that $\beta = \sigma_V^2/(kT_X/\mu m_H) \approx 1$ and that X-ray temperature and velocity dispersion are statistically measuring the same cluster property.

For the low values of the bias parameter ($b \approx 1.0$) that are implied by the large-scale normalization of the standard $\Omega = 1$ CDM scenario for structure formation this model appears to predict too many clusters with high velocity dispersions. Approximate agreement between observations and the $\Omega = 1$ CDM model can be obtained for bias parameters in the range $2 \lesssim b \lesssim 3$, in agreement with the earlier conclusions by FWED or White et al. (1993).

Acknowledgements. We thank Eelco van Kampen for helpful discussions and for allowing us to use his unpublished cluster models. Gavin Dalton is gratefully acknowledged for making available a machine-readable version of his Ph.D. thesis, as well as four alternative cluster catalogues based on the APM galaxy catalogue. We thank Mike West for providing us with his compilation of cluster redshifts. We thank the referee, L. Guzzo, for several useful comments and for pointing out an error in the manuscript, the correction of which has led to an important improvement of the paper. The cooperation between the members of the project was financially supported by the following organiza-

© European Southern Observatory • Provided by the NASA Astrophysics Data System

1996A&A...310...31M

tions: INSU, GR Cosmologie, Univ. de Provence, Univ. de Montpellier (France), CNRS-NWO (France and the Netherlands), Leiden Observatory, Leids Kerkhoven-Bosscha Fonds (the Netherlands), Univ. of Bologna, Univ. of Trieste (Italy), the Swiss National Science Foundation, the Ministerio de Educacion y Ciencia (Spain), CNRS-CSIC (France and Spain) and by the EC HCM programme.

References

Abell, G.O., 1958, ApJS, 3, 211
Abell, G.O., Corwin, H.G., Olowin, R.P., 1989, ApJS, 70, 1
Bahcall, N.A., Cen, R., 1992, ApJ, 398, L81
Bahcall, N.A., Soneira, R.M., 1983, ApJ, 270, 20
Beers, T.C., Flynn, K., Gebhardt, K., 1990, AJ, 100, 32
Biviano, A., Girardi, M., Giuricin, G., Mardirossian, F., Mezzetti, M., 1992, ApJ, 396, 35
Biviano, A., Girardi, M., Giuricin, G., Mardirossian, F., Mezzetti, M., 1993, ApJ 411, L13
Briel, U., Henry, G.P., 1993, A&A, 278, 379
Carlberg, R.G., 1994, ApJ, 433, 468
Collins, C.A., Guzzo, L., Nichol, R.C., Lumsden, S.L., 1995, MNRAS, 274, 1071
Dalton, G.B., 1992, PhD thesis, Oxford
Dalton, G.B., Efstathiou, G., Maddox, S.J., Sutherland, W.J., 1992, ApJ, 390, L1
Dalton, G.B., Efstathiou, G., Maddox, S.J., Sutherland, W.J., 1994, MNRAS, 269, 151
Danese, L., De Zotti, G., Di Tullio, G., 1980, A&A, 82, 322
Edge, A.C., Stewart, G.C., 1991, MNRAS, 252, 414
Edge, A.C., Stewart, G.C., Fabian, A., Arnaud, K.A., 1990, MNRAS, 245, 559
Efstathiou, G., Dalton, G.B., Sutherland, W.J., Maddox, S.J., 1992a, MNRAS, 257, 125
Efstathiou, G., Bond, J.R., White, S.D.M., 1992b, MNRAS, 258, 1p
Feldman, H.A., Kaiser, N., Peacock, J.A., 1994, ApJ, 426, 23
Frenk, C.S., White, S.D.M., Efstathiou, G., Davis, M., 1990, ApJ, 351, 10 (FWED)
Gerbal, D., Durret, F., Lachièze-Rey, M., 1994, A&A, 288, 746
Girardi, M., Biviano, A., Giuricin, G., Mardirossian, F., Mezzetti, M., 1993, ApJ, 404, 38
den Hartog, R.H., Katgert, P., 1995, submitted to MNRAS
Henry, J.P., Arnaud, K.A., 1991, ApJ, 372, 410
Katgert, P., Mazure, A., Perea, J., et al., 1995,TO BE FILLED IN BY EDITOR AANDA
Katz, N., Hernquist, L., Weinberg, D.W., 1992, ApJ, 399, L109
Katz, N., Quinn, T., Bertschinger, E., Gelb, J.M., 1994, MNRAS, 270, L71
Lubin, L.M., Bahcall, N.A., 1993, ApJ, 415, L17
Lumsden, S.L., Nichol, R.C., Collins, C.A., Guzzo, L., 1992, MNRAS, 258, 1 (LNCG)
Metzler, C., Evrard, A., 1994, ApJ, 437, 564
Peacock, J.A., West. M.J., 1992, MNRAS, 259, 494
Pierre, M., Bohringer, H., Ebeling,H., et al., 1994, A&A, 290, 725
Postman, M., Huchra, J.P., Geller, M.J., 1992, ApJ, 384, 404
Quintana, H.R., Ramírez, A., 1995, ApJS, 96, 343
Scaramella, R., Zamorani, G., Vettolani, G., Chincarini, G., 1991, AJ, 101, 342
Seljak, U., Bertschinger, E., 1994, ApJ, 427, 523
Struble, M.F., Rood, H.J., 1991, ApJS, 77, 363
Summers, F.J., 1993, PhD thesis, Berkeley
Van Kampen, E., 1994, PhD thesis, Leiden Observatory
Van Kampen, E., 1995, MNRAS, 273, 295
Van de Weygaert, R., Babul, A., 1994, ApJ, 425, L59
Walsh, D., Miralda-Escudé, J., 1995, MNRAS, in press
White, S.D.M., Efstathiou, G., Frenk, C.S., 1993, MNRAS, 262, 1023
Wright, E.L., Meyer, S.S., Bennett, C.L., Boggess, N.W., et al. 1992, ApJ, 396, L13
Zabludoff, A.I., Geller, M.J., Huchra, J.P., Ramella, M., 1993, AJ, 106, 1301 (ZGHR)

This article was processed by the author using Springer-Verlag LaTeX A&A style file version 3.

© European Southern Observatory • Provided by the NASA Astrophysics Data System